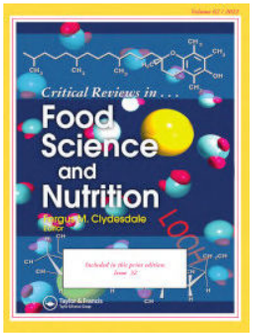

Taylor & Francis
Taylor & Francis Group

Critical Reviews in Food Science and Nutrition

ISSN: (Print) (Online) Journal homepage: https://www.tandfonline.com/loi/bfsn20

An advantageous application of molecularly imprinted polymers in food processing and quality control

Viknasvarri Ayerdurai, Patrycja Lach, Agnieszka Lis-Cieplak, Maciej Cieplak, Wlodzimierz Kutner & Piyush Sindhu Sharma

To cite this article: Viknasvarri Ayerdurai, Patrycja Lach, Agnieszka Lis-Cieplak, Maciej Cieplak, Wlodzimierz Kutner & Piyush Sindhu Sharma (2022): An advantageous application of molecularly imprinted polymers in food processing and quality control, Critical Reviews in Food Science and Nutrition, DOI: 10.1080/10408398.2022.2132208

To link to this article: https://doi.org/10.1080/10408398.2022.2132208

Published online: 27 Oct 2022.

CRITICAL REVIEWS IN FOOD SCIENCE AND NUTRITION
https://doi.org/10.1080/10408398.2022.2132208

Taylor & Francis
Taylor & Francis Group

REVIEW

An advantageous application of molecularly imprinted polymers in food processing and quality control

Viknasvarri Ayerdurai[a*], Patrycja Lach[a*], Agnieszka Lis-Cieplak[b], Maciej Cieplak[a], Wlodzimierz Kutner[a,c] and Piyush Sindhu Sharma[a]

[a]Institute of Physical Chemistry, Polish Academy of Sciences, Warsaw, Poland; [b]Faculty of Pharmacy, Medical University of Warsaw, Warsaw, Poland; [c]Faculty of Mathematics and Natural Sciences, School of Sciences, Cardinal Stefan Wyszynski University in Warsaw, Warsaw, Poland

ABSTRACT

In the global market era, food product control is very challenging. It is impossible to track and control all production and delivery chains not only for regular customers but also for the State Sanitary Inspections. Certified laboratories currently use accurate food safety and quality inspection methods. However, these methods are very laborious and costly. The present review highlights the need to develop fast, robust, and cost-effective analytical assays to determine food contamination. Application of the molecularly imprinted polymers (MIPs) as selective recognition units for chemosensors' fabrication was herein explored. MIPs enable fast and inexpensive electrochemical and optical transduction, significantly improving detectability, sensitivity, and selectivity. MIPs compromise durability of synthetic materials with a high affinity to target analytes and selectivity of molecular recognition. Imprinted molecular cavities, present in MIPs structure, are complementary to the target analyte molecules in terms of size, shape, and location of recognizing sites. They perfectly mimic natural molecular recognition. The present review article critically covers MIPs' applications in selective assays for a wide range of food products. Moreover, numerous potential applications of MIPs in the food industry, including sample pretreatment before analysis, removal of contaminants, or extraction of high-value ingredients, are discussed.

KEYWORDS

Molecularly imprinted polymer; electrochemical chemosensor; optical chemosensor; food analysis; food toxin

1. Introduction

There is no healthy diet without healthy food. Therefore, the modern lifestyle requires easy access to high-quality food products (Wijayaratne et al. 2018). On the one hand, this trend supports the sustainable development of agricultural production and returns it to the traditional cultivation methods (Antonelli and Viganò 2018). On the other hand, it boosts the import of food products from exotic destinations. Both trends significantly increase production and delivery costs, while market competition enforces low-price maintenance. That tempts dishonest producers and suppliers (Soon et al. 2019; Ali and Suleiman 2018). Therefore, food product quality should be controlled at various manufacturing and distributing stages.

This control is very challenging in the global market era (Soon et al. 2019; Ali and Suleiman 2018). It is nearly impossible to track and control all food production and delivery chains not only for regular customers but also for the State Sanitary Inspections. Therefore, food manufacturers would try to unfairly raise the quantity and quality of the manufactured products (Silva et al. 2021). Furthermore, different chemicals used during farming, i.e., chemical fertilizers, pesticides, herbicides, antibiotics, antifungals, hormones, and food additives used by the food industry, including food preservatives, dyes, and artificial fragrances, can be present in food in significant amounts. Moreover, food products may be accidentally contaminated with heavy metal ions and toxins of industrial or natural origin. These toxins may be produced by mold or bacteria during food rotting. All of the above have adverse effects on the consumers' health.

Currently, certified laboratories are using accurate food quality and safety analysis methods. However, these methods are usually very laborious. They require well-trained and experienced employees and, frequently, costly instrumentation, e.g., high-performance liquid chromatography with mass spectrometry detection (HPLC-MS) (Silva et al. 2018). Therefore, the need to develop fast, robust and cost-effective analytical assays to determine food product contaminants should be highlighted. Moreover, newly developed analytical methods should easily be integrated with portable, hand-held devices, thus enabling on-spot sample analysis (Nelis et al. 2020).

Numerous electrochemical and optical methods of analytical signal transduction perfectly fulfill these requirements. However, their sensitivity and especially selectivity are far insufficient for successful sensors devising. Integrating selective recognizing units with the signal's transducer is

CONTACT Wlodzimierz Kutner wkutner@ichf.edu.pl; Maciej Cieplak mcieplak@ichf.edu.pl
*Contribution of both Authors was equal.

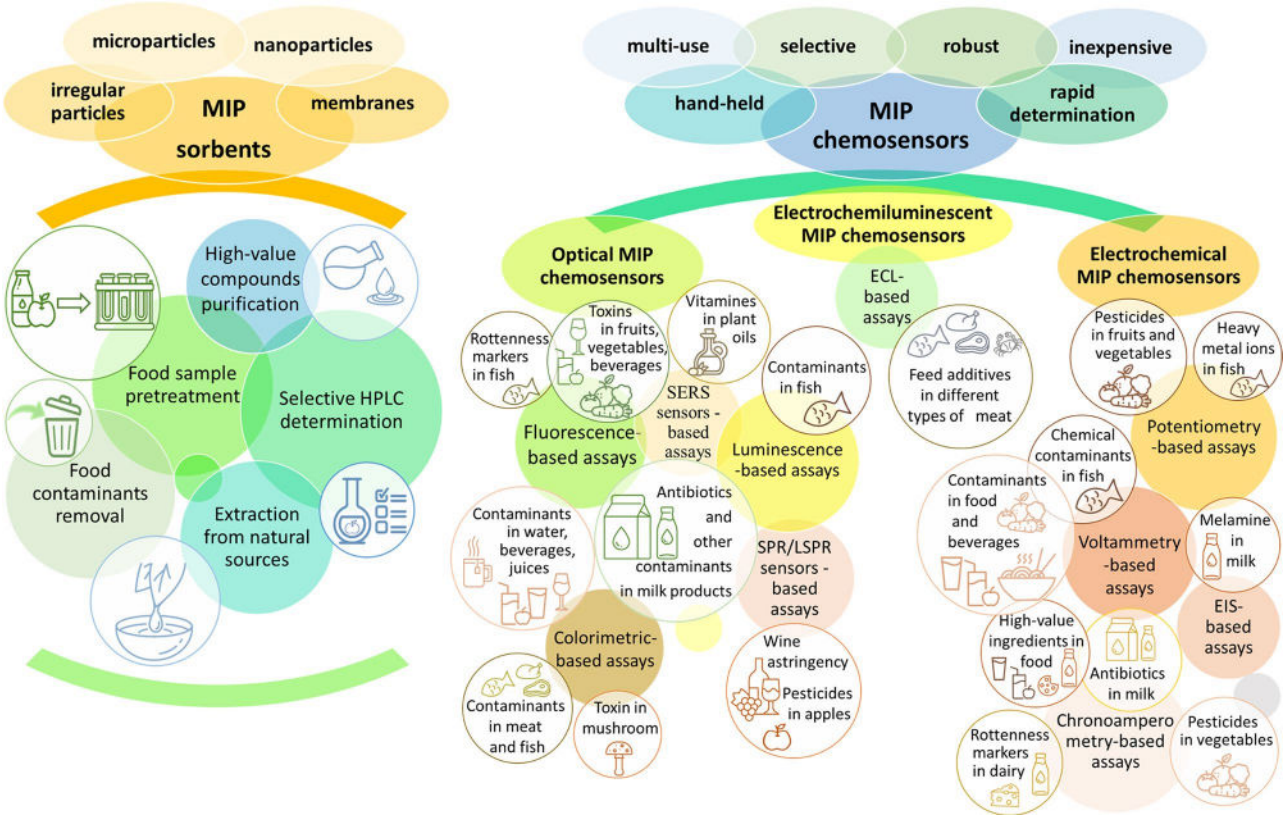

Scheme 1. Outline of MIPs applications in the food industry and food quality control protocols.

necessary to circumvent this deficiency (Khanmohammadi et al. 2020; Naresh and Lee 2021; Chen and Wang 2020). Applying biological recognizing units, including DNAs, aptamers, enzymes, monoclonal antibodies, cells, or even whole tissues, opened a route to devise various biosensors. Biosensors are sensitive and highly selective, and often specific. Therefore, abundant biosensors found their way to the market. Glucometers and pregnancy tests are the most widely offered biosensors. Despite their advantages, they suffer from several drawbacks. Their low durability originates from components of the biological origin. Therefore, they mostly serve as disposable devices. Alternately, e.g., multi-use glucometers require single-use sensing stripes with the glucose oxidase (GOx) or glucose dehydrogenase (GDH) enzyme immobilized on their surface. Such a cost-ineffective and high-waste approach may be accepted only in the healthcare field. More cost-effective sensors are in demand in food analysis, especially for controlling industrial-scale food production. For that purpose, chemically synthesized receptors may be immobilized on the transducer surface. Macrocyclic compounds, including cyclodextrins, crown ethers, and calixarenes, offer much better durability but at the expense of selectivity much lower than that of the bioreceptors.

Molecularly imprinted polymers (MIPs) compromise the durability of synthetic sensing materials with a high affinity to target analytes and selectivity of molecular recognition (Cieplak and Kutner 2016). Therefore, they effectively mimic natural molecular recognition. The present review critically covers the MIPs applications in chemosensors devised for selective food analysis using various transduction techniques and a wide range of tested products. Moreover, numerous potential applications of MIPs in the food industry, including sample pretreatment before analysis, removal of contaminants, or extraction of high-value ingredients, are discussed (Scheme 1).

2. Molecularly imprinted polymers (MIPs)

MIPs are an illustrative example of nature-inspired smart materials (Cieplak and Kutner 2016). In their matrices, MIPs contain molecular cavities imprinted during polymerization. For that purpose, template molecules are added to the solution for polymerization. Then, the polymer grows around these molecules during the polymerization. Later, these molecules' removal results in molecular cavities in the polymer structure, resembling template molecules with their shape, size, and orientation of recognizing sites. These cavities can recognize and capture only these molecules that spatially fit them. Moreover, carefully selected monomers, called functional monomers, are used for polymerization to increase the selectivity of this molecular recognition. These monomers contain recognition sites, including functional groups, heteroatoms, π-π conjugated systems, etc., that interact with binding sites of template molecules via covalent bonds, hydrogen bonds, electrostatic attractions, π-π stacking, as well as hydrophobic and van der Walls interactions (Scheme 2). These monomers form stable pre-polymerization complexes with template molecules in solution; thus, they are

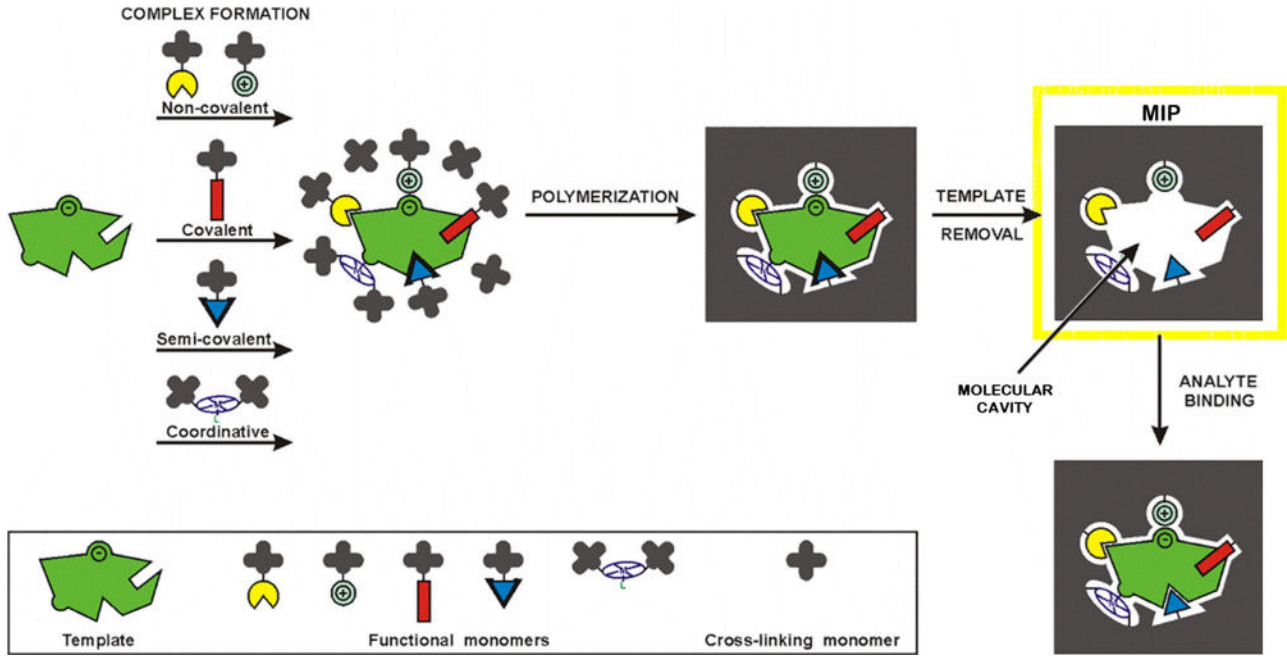

Scheme 2. The flowchart of a general procedure of MIP synthesis. Adapted from Sharma et al. (2013).

built into the growing polymer during the polymerization. After template removal from the MIP, they stay as recognizing sites on the walls of the imprinted cavities, increasing the affinity of these cavities to the target analyte molecules and thus the binding selectivity.

Depending on their potential applications, MIPs are synthesized in many different forms, including bulk polymers, membranes, grains, micro- and nanoparticles (NPs), or thin films grafted on the solid support surfaces of diverse morphology. Several different polymerization procedures were employed for synthesizing MIPs, ranging from simple light-inducted free radical polymerization through emulsion polymerization and "living" polymerization to electrochemical polymerization. Details of MIPs synthesizing and characterizing have already been reported in various high-quality review articles (Uzun and Turner 2016; Wackerlig and Lieberzeit 2015; Niu, Chuong, and He 2016; Sharma et al. 2013; Beyazit et al. 2016). The readers who wish to explore the basics of molecular imprinting are encouraged to get acquainted with these articles. The present article focuses on the existing or potential applications of MIPs in food production and selective MIP chemosensors devised for food products analysis.

3. MIP sorbents application in food processing and control

The most common MIPs applications are separation materials where an unusually high degree of selectivity of the sorbents is utilized. For that, MIPs can be synthesized as irregular or spherical micro- or nanoparticles, membranes, or bulk materials that can be ground later. Prepared that way, MIPs may be used for dispersion extraction or as packing materials for solid-phase extraction (SPE) cartridges and high-performance liquid chromatography (HPLC) columns. The fast-growing field of MIP sorbents was reviewed in detail elsewhere (Turiel and Martin-Esteban 2010; Ashley et al. 2017). MIP-based separation materials are very convenient for sample preparation and purification. This opens up new opportunities for the food industry. Recently, several companies were established to develop and introduce MIP sorbents to the market. Only commercial examples are discussed in this chapter.

3.1. MIP SPE cartridges for sample pretreatment before food sample analysis

Developing new analytical methods for food product control and analysis may be a tremendous task. Usually, food products are inhomogeneous. They represent a complicated mixture of many different components in various concentration ranges. The analyte of interest may often be present in the analyzed sample at a concentration of several orders of magnitude lower than the interferences. Moreover, the HPLC system with a simple UV-vis or refractive index detection requires a relatively high analyte concentration. Therefore, food samples usually need laborious and time-consuming pretreatments to pre-concentrate the analyte and partially remove interferences that may foul and thus destroy the HPLC column. Hence, MIP sorbing materials appeared very useful in preliminary sample preparation procedures for HPLC assays (Scheme 3a). Recently, numerous MIP-SPE/HPLC resins were commercialized (Table 1). Mainly, they are dedicated to clinical analysis. However, examples of MIP-SPE/HPLC resins application to food analysis were also reported.

In the preceding decade, the NanoMyP® company introduced two types of MIP microparticles, commercialized as a dry powder, for selective extraction of ascorbic acid (Valero-Navarro et al. 2011) and tetracyclines via dispersion

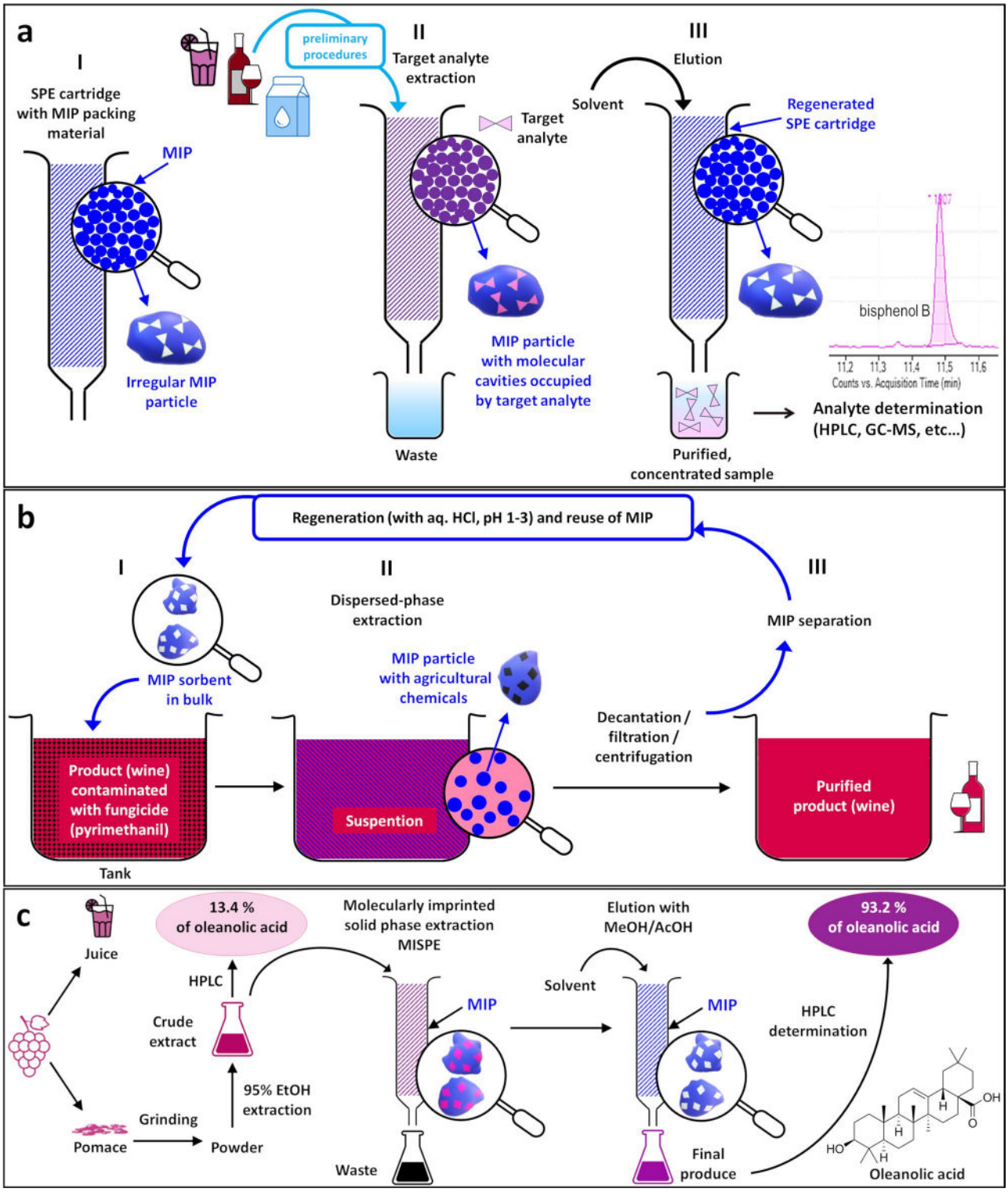

Scheme 3. (a) Food sample pretreatment before sample analysis. An example of ochratoxin A (OTA) HPLC determination in beer, red wine, and grape juice samples (Cao, Kong, et al. 2013) and GC-MS determination of bisphenol compounds in breast milk samples (Deceuninck et al. 2015). (b) Removal of food contaminants during processing. Purification of wine contaminated with pyrimethanil (Petcu 2013, 2015). (c) High-value compounds extraction. Molecularly imprinted SPE of oleanolic acid from grape pomace extract (Lu et al. 2018).

extraction. Moreover, the former resin was packed into an HPLC column and applied for selective ascorbic acid determination in fruit juice. Then, two more companies, namely POLYINTELL (AFFINISEP) and Merck (SupelMIP), offered several ready-to-use SPE cartridges. Their applications appeared to be useful for selectivity improvement in HPLC determination of mycotoxins (Catana et al. 2019; Cao, Zhou, et al. 2013; Cao, Kong, et al. 2013; Gonzalez-Salamo et al. 2015; Bryła et al. 2013; Lucci et al. 2010), antibiotics (Blasco and Pico 2012; Cirkva et al. 2019; Bustamante-Rangel, Rodríguez-Gonzalo, and Delgado-Zamareño 2022), bisphenols (Matejicek, Grycova, and Vlcek 2013; Deceuninck et al.

Table 1. Commercial solid-phase extraction (SPE) columns and their application in the food industry.

	Commercial MIP			Details of application				
No.	Company	Product type	Product name	Type of application	Group of contaminants	Specific target	Food product	Ref.
1	NanoMyP	Resin for SPE/HPLC in the form of dry 5 µm particles	CA-MIP	Extraction/Selective HPLC determination	Naturally-occurring antioxidant	Caffeic acid		(Valero-Navarro et al. 2011)
2	NanoMyP	Resin for SPE/HPLC in the form of dry 1 µm particles	TTC-MIP	Extraction/Selective HPLC determination	Antibiotics	Tetracycline	–	–
3	AFFINISEP (POLYINTELL)	SPE column	AFFINIMIP® SPE Patulin	Sample pretreatment before chromatographic analysis	Mycotoxins	Patulin	Apple juice (clear & cloudy), apple and multifruit puree, baby food, cider (Catana et al. 2019), alcohol, Pommeau, dried apple, blueberry, tomato ketchup	(Catana et al. 2019)
4	AFFINISEP (POLYINTELL)	SPE column	AFFINIMIP® SPE Ochratoxin A	Sample pretreatment before chromatographic analysis	Mycotoxins	Ochratoxin A	Wheat, maize, wine (Cao, Kong, et al. 2013), beer (Cao, Kong, et al. 2013), grape juice (Cao, Kong, et al. 2013), spices, i.e., paprika, pepper, ginger (Cao, Zhou, et al. 2013), cocoa, etc.	(Cao, Zhou, et al. 2013; Cao, Kong, et al. 2013)
5	AFFINISEP (POLYINTELL)	SPE column	AFFINIMIP® SPE Zearalenone	Sample pretreatment before chromatographic analysis	Mycotoxins	Zearalenone, α-zeranol, and β-zeranol	Water (Gonzalez-Salamo et al. 2015), wheat, maize, cereal-based baby food, corn oil, and rice	(Gonzalez-Salamo et al. 2015)
6	AFFINISEP (POLYINTELL)	SPE column	AFFINIMIP® SPE Fumonisins	Sample pretreatment before chromatographic analysis	Mycotoxins	Fumonisins	–	–
7	AFFINISEP (POLYINTELL)	SPE column	AFFINIMIP® SPE Deoxynivalenol	Sample pretreatment before chromatographic analysis	Mycotoxins	Deoxynivalenol (vomitoxin), 3-acetylDON, and 15-acetylDON	Oat, wheat, corn, baby food, meat, animal feed, etc.	–
8	AFFINISEP (POLYINTELL)	SPE column	AFFINIMIP® SPE Aflatoxine	Sample pretreatment before chromatographic analysis	Mycotoxins	Aflatoxin	–	–
9	AFFINISEP (POLYINTELL)	SPE column	AFFINIMIP® SPE FumoZON	Sample pretreatment before chromatographic analysis	Mycotoxins	Fumonisins B_1/B_2 (Bryła et al. 2013), and zearalenone (Lucci et al. 2010)		(Bryła et al. 2013; Lucci et al. 2010)

(*Continued*)

Table 1. (Continued).

No.	Commercial MIP			Details of application				Ref.
	Company	Product type	Product name	Type of application	Group of contaminants	Specific target	Food product	
10	AFFINISEP (POLYINTELL)	SPE column	AFFINIMIP® SPE MultimycoLCMSMS	Sample pretreatment before chromatographic analysis	Mycotoxins	Fumonisins B1/B2, aflatoxins B1/B2/G1/G2, ochratoxin A, T-2, HT-2, zearalenone, and deoxynivalenol	Wheat, maize, cereals, sunflower seeds, etc.	–
11	AFFINISEP (POLYINTELL)	SPE column	AFFINIMIP® SPE Glyphosate	Sample pretreatment before chromatographic analysis	Herbicides	Glyphosate, AMPA, and glufosinate	Water, cereal, honey, tea, juices, and cannabis	–
12	AFFINISEP (POLYINTELL)	SPE column	AFFINIMIP® SPE Picolinic	Sample pretreatment before chromatographic analysis	Herbicides	Picloram, aminopyralid, and clopyralid	Water, compost, cereal, soil, etc.	–
13	AFFINISEP (POLYINTELL)	SPE column	AFFINIMIP® SPE PAHs	Sample pretreatment before chromatographic analysis	PAHs	Bezno[a]antracen, benzo[a]pyren, benzo[a]fluoranthen, chrysen, etc.	Oils and fatty food	–
14	AFFINISEP (POLYINTELL)	SPE column	AFFINIMIP® SPE Tetracyclines	Sample pretreatment before chromatographic analysis	Antibiotics	Tetracycline, chlortetracycline, oxytetracycline, and doxycycline	Meat and milk	–
15	AFFINISEP (POLYINTELL)	SPE column	AFFINIMIP® SPE Chloramphenicol	Sample pretreatment before chromatographic analysis	Antibiotics	Chloramphenicol	Honey, milk, shrimp, and bovine urine	–
16	AFFINISEP (POLYINTELL)	SPE column	AFFINIMIP® SPE Aminoglycosides	Sample pretreatment before chromatographic analysis	Antibiotics	Spectinomycin, hygromycin B, streptomycin, dihydrostreptomycin, amikacin, kanamycin A, apramycin, paromomycin, tobramycin, sisomicin, gentamicin C1a/C2, neomycin B	Tissues muscles, milk, fish, egg	–
17	AFFINISEP (POLYINTELL)	SPE column	AFFINIMIP® SPE Bisphenols	Sample pretreatment before chromatographic analysis	Bisphenols	Bisphenol A and closely 18 related structures	Water (Matejicek, Grycova, and Vlcek 2013), milk (infant formula), human breast milk (Deceuninck et al. 2015), canned food, vegetable puree for infants, beer, pineapple (Kubiak, Ciric, and Biesaga 2020), lentil (Kubiak, Ciric, and Biesaga 2020), bean (Kubiak, Ciric, and Biesaga 2020), etc.	(Matejicek, Grycova, and Vlcek 2013; Deceuninck et al. 2015; Kubiak, Ciric, and Biesaga 2020)
18	AFFINISEP (POLYINTELL)	SPE column	AFFINIMIP® SPE Zeranol	Sample pretreatment before chromatographic analysis	Antibiotics	Zeranol, zearalenone, taleranol, Zearalenol α/β, zearalanone, and resorcynic acid lactones	Meat, urine, tissues, and plasma	–

19	AFFINISEP (POLYINTELL)	SPE column	AFFINIMIP® SPE Phenolics	Sample pretreatment before chromatographic analysis	Phenolic compounds	Parabens, carnosic acid, hydroxylated PAHs, tocopherols, nitrophenols, chloro-/bromophenols (Roszko, Szymczyk, and Jędrzejczak 2015), catechins, estriols (Bousoumah et al. 2015), bisphenols (Bousoumah et al. 2015; Nicolucci et al. 2013; Matejicek, Grycova, and Vlcek 2013), coumarin (Hrobonova and Brokesova 2020), etc.		(Matejicek, Grycova, and Vlcek 2013; Bousoumah et al. 2015; Nicolucci et al. 2013; Roszko, Szymczyk, and Jędrzejczak 2015; Hrobonova and Brokesova 2020)
20	Merck	SPE column	SupelMIP® SPE—Patulin	Sample pretreatment before chromatographic analysis	Mycotoxins	Patulin	–	–
21	Merck	SPE column	SupelMIP® SPE—Bisphenol A	Sample pretreatment before chromatographic analysis	Bisphenols	Bisphenol A	–	–
22	Merck	SPE column	SupelMIP® SPE—Aminoglycosides	Sample pretreatment before chromatographic analysis	Antibiotics	Dihydrostreptomycin, streptomycin, tobramycin, kanamycin, amikacin, gentamicin, neomycin, apramycin, spectinomycin, and hygromycin B	–	–
23	Merck	SPE column	SupelMIP® SPE—Riboflavin (vitamin B2)	Sample pretreatment before chromatographic analysis	Vitamins	Vitamin B2	Milk	–
24	Merck	SPE column	SupelMIP® SPE—Chloramphenicol	Sample pretreatment before chromatographic analysis	Antibiotics	Chloramphenicol	–	–
25	Merck	SPE column	SupelMIP® SPE—Fluoroquinolones	Sample pretreatment before chromatographic analysis	Antibiotics	Sarafloxacin, norfloxacin, enrofloxacin, and ciprofloxacin		(Blasco and Pico 2012)
26	Merck	SPE column	SupelMIP® SPE—Nitroimidazoles	Sample pretreatment before chromatographic analysis	Antibiotics	Dimetridazole, ipronidazole, metronidazole, ronidazole, and their hydroxylated metabolites (Cirkva et al. 2019); Numerous nitroimidazoles and benzimidazoles (Bustamante-Rangel, Rodríguez-Gonzalo, and Delgado-Zamareño 2022)		(Cirkva et al. 2019; Bustamante-Rangel, Rodríguez-Gonzalo, and Delgado-Zamareño 2022)
27	Ligar Ltd. Partnership (previously Ligar Polymers Ltd.)	SPE cartridge	Not specified	Removal	Fungicide	Pyrimethanil: a fungicide widely used in treating grapevines.	Wine (Petcu 2013, 2015)	US 20150361203 (Petcu 2015) and WO 2013190506 (Petcu 2013)

2015; Kubiak, Ciric, and Biesaga 2020; Bousoumah et al. 2015; Nicolucci et al. 2013), and other contaminants (Roszko, Szymczyk, and Jędrzejczak 2015; Hrobonova and Brokesova 2020) in water (Gonzalez-Salamo et al. 2015; Matejicek, Grycova, and Vlcek 2013), cider (Catana et al. 2019), wine (Cao, Kong, et al. 2013; Hrobonova and Brokesova 2020), beer (Cao, Kong, et al. 2013), grape juice (Cao, Kong, et al. 2013), cereal (Bryła et al. 2013; Lucci et al. 2010), pineapple (Kubiak, Ciric, and Biesaga 2020), lentil (Kubiak, Ciric, and Biesaga 2020), bean (Kubiak, Ciric, and Biesaga 2020), ginger (Cao, Zhou, et al. 2013), eggs (Blasco and Pico 2012), and meat products (Roszko, Szymczyk, and Jędrzejczak 2015; Cirkva et al. 2019).

3.2. Undesired ingredients removal from food products

Another possible application of MIP resins is the selective removal of undesired ingredients from food products. For that, a Ligar PL company was established in New Zealand to devise and fabricate MIPs to remove harmful food contaminants, including heavy metal ions or pesticides that may be extracted from liquid food products, i.e., drinking water, wine, cooking oil, or juice. Moreover, bitter, smoker, and unpleasant tastes or flavors may be removed from these products without significant loss of their desired properties. However, until now, this company has only presented successful removal of pyrimethanil fungicide from wine (Scheme 3b) (Petcu 2013, 2015). Ligar PL products have not yet been introduced to the worldwide market. But a high application potential of the purification procedure developed may be illustrated by MIP particles successfully devised by the K. Haupt group, in cooperation with the L'Oréal company, to remove odorous components of human sweat (Nestora et al. 2016; Mier et al. 2019).

3.3. Desired compounds extraction from natural sources

The under-estimated but presumably potentially the most profitable application of MIP particles is a selective extraction of high-value compounds from natural sources. Toward that, MIP particles can be dispersed in natural mixtures to absorb desired ingredients and then readily separated by sedimentation, filtration, centrifugation, or by applying a magnetic field in the case of magnetic MIP NPs (da Fonseca Alves et al. 2021; Aylaz et al. 2021). Therefore, this extraction may be performed under continuous-flow conditions, even on an industrial scale. In one important example, the G. Szekely group demonstrated extensive optimization of MIP particles synthesis and regeneration procedures (Kupai et al. 2017). Different L-phenylalanine methyl ester imprinted MIP particles were subjected to 100 adsorption-regeneration cycles. There was no loss of binding capacity within these 100 cycles for all examined MIP particles, even if the process was performed at elevated temperature (65 °C) and if methanol was used as the solvent for particle regeneration. Moreover, if divinyl benzene was applied as the cross-linking monomer, MIP particles' binding capacity was unaffected by regeneration neither in acidic nor basic aqueous solution during all 100 cycles. However, MIP particles synthesized with ethylene glycol dimethacrylate or *N*,*N*'-methylenebis(acrylamide) cross-linking monomers deteriorated after the first 20 sorption-regeneration cycles. Therefore, applying MIP particles for selective extraction seems economically justified if considering high extraction selectivity and potentially low cost of the MIP particles' synthesis. Accordingly, extraction of rosmarinic acid (Zahara et al. 2021) and quercetin (Pakade et al. 2013), as well as kaempferol (Pakade et al. 2013) from 3 kg of dried Salvia hypoleuca (Zahara et al. 2021) and 5 g of dried Moringa oleifera leaves (Pakade et al. 2013) were demonstrated, respectively. Moreover, in another example oleanolic acid imprinted polymer was applied to extract this acid from 150 mg grape pomace extract (Scheme 3c) (Lu et al. 2018). After the purification using MIP loaded column, the content of oleanolic acid increased from 13.4% to 93.2%. Unfortunately, these procedures were performed only on the laboratory scale and have not been scaled up yet. Recently, Ligar PL has established a new daughter company, Amber Purification Ltd., devoted to developing a large-scale system to purify cannabinoid extracts from hemp. However, their products have not been commercialized yet.

4. MIP chemosensors for food products analysis

The HPLC assays mentioned above enable very selective and reproducible contaminants determination in food samples, thus ensuring highly reliable food quality control. However, these assays suffer from several disadvantages. They use high quantities of expensive solvents of very high purity. With the unit price exceeding 100,000 EUR, an HPLC system equipped with a mass spectrometry detector is mainly supplied to sanitary inspection laboratories and industrial-scale food manufacturers. It is inaccessible for small food manufacturers, not to mention individual farmers and food market customers. Importantly, these systems are unsuitable for in-field determinations. Therefore, all examined samples must be collected and transported to specialized laboratories. That highlights the urge to design inexpensive, hand-held chemosensors for fast and straightforward analyte determinations. The following sections describe the MIP chemosensors' application for various food sample testing, including determining particular contaminants or other relevant compounds. The most critical analysis details, the techniques used, and the food sample types are summarized in Tables 2 and 3.

4.1. MIP chemosensors for optical assays

Optical sensors are robust and inexpensive. For many procedures, optical assays are designed to give a readout that can be recorded by the naked eye of the operator, i.e., by observing color changes caused by the characteristic color reaction. MIPs may provide analyte preconcentration and selectivity enhancement for these procedures (Ye et al. 2018; Wu et al. 2018; Zhao et al. 2019; Feng et al. 2017).

Table 2. Examples of MIPs application for optical sensing in food samples.

No.	Group of contaminants	Specific target	Details of MIP sensing protocol	Type of assay	Dynamic linear concentration range	LOD	Naked eye detection	Food product analyzed	Ref.
1	Pesticide	3-Phenoxybenzaldehyde, a metabolite of pyrethroid	Imprinted silica particles were applied for preconcentration of the analyte before a characteristic color-changing reaction with potassium permanganate	Colorimetric	0.1–1 μg mL^{-1}	0.052 μg mL^{-1}	Yes	River water, fruit juice, and beverage	(Ye et al. 2018)
2	Insecticide	Cartap	Magnetic MIP particles were applied for preconcentration of the analyte before a colorimetric assay based on Ag NPs localized plasmon resonance	Colorimetric	0.1–5 mg L^{-1}	0.01 mg L^{-1}	Yes, 0.1–5 mg L^{-1}	Tea beverage	(Wu et al. 2018)
3	Herbicide	Atrazine	MIP particles were applied for preconcentration of the analyte before the assay	Colorimetric	0.005–1 mg L^{-1}	50 μg L^{-1}	Yes	Apple juice	(Zhao et al. 2019)
4				SERS	0.005–1 mg L^{-1}	1.2 μg L^{-1}	–		
5	Insecticide	Chlorpyrifos	MIP particles were applied for preconcentration of the analyte before the assay	Colorimetric	0.1–10 mg L^{-1} [a]	–	Yes	Apple juice	(Feng et al. 2017)
6				SERS	0.01–1 mg L^{-1}	–	–		
7	Necessary nutrients	α-Tocopherol (a component of Vitamin E)	MIP particles were applied for preconcentration of the analyte before the assay	SERS	2–20 mg g^{-1}	–	–	Peanut oil, olive oil, corn oil, and canola oil	(Feng et al. 2013)
8	Toxin	Ethyl carbamate	MIP particles were applied for preconcentration of the analyte before the assay	SERS	0.1–0.5 mg L^{-1}	–	–	Rice wine and fruit brandy	(Wu et al. 2016)
9	Herbicide	2,4-Dichlorophenoxyacetic acid	MIP particles were applied for preconcentration of the analyte before the assay	SERS	0.01–1 ppm	0.006 ppm	–	Milk	(Hua et al. 2018)
10	Fungicide	Thiabendazole	MIP particles were applied for preconcentration of the analyte before the assay	SERS	10–75 ppm	4 ppm	–	Orange juice	(Feng et al. 2018)

(*Continued*)

Table 2. (Continued).

No.	Group of contaminants	Specific target	Details of MIP sensing protocol	Type of assay	Dynamic linear concentration range	LOD	Naked eye detection	Food product analyzed	Ref.
11	Biogenic amines signaling food rottenness	Histamine	MIP particles were applied for preconcentration of the analyte before the assay. The analyte was extracted from MIP with Au NPs solution	SERS	3–90 ppm	–	–	Canned tuna	(Gao, Grant, and Lu 2015)
12	Antibiotic	Chloramphenicol	MIP decorated with Au NPs	SERS	0.1–50 μg mL^{-1}	0.1 μg mL^{-1}	–	Milk	(Xie et al. 2017)
13	Chemical contamination	Melamine	MIP decorated with Ag NPs	SERS	0.01–0.1 mM	16.5 μM	–	Milk	(Hu and Lu 2016)
14	Necessary nutrients	L-Phenylalanine	MIP film grafted on the Au NPs	SERS	1.0×10^{-4}–1.0×10^{-8} M [b]	1 nM	–	Bovine serum	(Zhou et al. 2020)
15	Chemical contamination	Sudan I	MIP microparticles served as stationary phase for TLC and were decorated with Au NPs	SERS	1–100 ppm	1 ppm	–	Paprika powder	(Gao et al. 2015)
16	Chemical contamination	Bisphenol A	Imprinted silica was grafted on SiO_2@Ag NPs	SERS	1.75×10^{-11}–1.75×10^{-6} M [b]	1.46×10^{-11} M	–	Milk	(Yin, Wu, et al. 2018)
17	Dye	Rhodamine 6G	Ordered Au NPs monolayer was incorporated into inverse opal macroporous MIP	SERS	10^{-10}–10^{-4} M [b]	10^{-10}	–	Orange juice	(Wang et al. 2020)
18	Insecticide	Imidacloprid	Paper substrate was covered with carbon ink on one side, and silver dendrites were deposited on the other by chemical reduction. Polypyrrole MIP was deposited via electropolymerization. Finally, MIP was decorated with Ag NPs by chemical reduction of silver nitrate	SERS	0.2–800 ng mL^{-1}	0.028 ng mL^{-1}	–	Chinese chives, crown daisy, soybean, and cucumber	(Zhao, Liu, et al. 2020)
19	Biogenic amines signaling food rottenness	Histamine	MIP film was grafted with free-radical polymerization on the surface of ZnO@ TiO_2@Ag NPs	SERS	10 nM–1 mM	3.1 nM	–	Liquor, vinegar, and prawn	(Chen, Wang, et al. 2022)

20	Biogenic amines signaling food rottenness	Histamine	Competitive absorption assay between histamine and fluorescent BODIPY® FL Histamine	Fluorescence	1–430 μM [a]	–	–	Fish	(Mattsson et al. 2018)
21	Pesticide	Cyhalothrin	Fluorescent MIP particles containing co-polymerized allyl fluorescein	Fluorescence	0–1.0 nM	4 pM	–	Honey	(Gao, Li, et al. 2014)
22	Fungicide	Fenaminosulf	ITO transparent electrode coated with the Ag film and the MIP film using electropolymerization. Fluorescent neutral red-labeled hydroquinone serving as the functional monomer	Fluorescence	2×10^{-10}–4×10^{-8} M	1.6×10^{-11} M	–	Lettuce, cabbage, tomato, and banana	(Li, Yin, et al. 2015)
23	Biogenic amines signaling food rottenness	Histamine	MIP film grafted on fluorescent CdSe/ZnS QDs	Fluorescence	0.449–2.249 mM	0.11 mM	–	Fish can samples (trout, tuna, sardine, saury cans)	(Wang, Fang, et al. 2017)
24	Dye	Malachite green	MIP film grafted on fluorescent CdTe QDs	Fluorescence	0.1–20 μM	59 nM	–	Fish	(Wu, Lin, et al. 2017)
25	Antibiotic	Doxycycline	Fluorescent MIP particles containing co-polymerized fluorescein-*O*-acrylate	Fluorescence	0.2–6 μM	117 nM	–	Pork plasma	(Ashley, Feng, and Sun 2018)
26	Toxin	Saxitoxin, a paralytic shellfish toxin	Imprinted silica film grafted on fluorescent CdS/CdSe/ZnS QDs	Fluorescence	20–100 μg L^{-1}	0.3 μg kg^{-1}	–	Shellfish	(Sun et al. 2018)
27	Insecticide	Cyfluthrin	Imprinted silica film grafted on fluorescent FeSe QDs	Fluorescence	10–200 μg L^{-1}	1 μg kg^{-1}	–	Fish	(Li, Jiao, et al. 2018)
28	Chemical contamination	3-Monochloropropane-1,2-diol	MIP grafted with free-radical polymerization on filter paper decorated with carbon QDs	Fluorescence	1–150 ng mL^{-1}	0.6 ng mL^{-1}	Yes	Soy sauce	(Fang et al. 2019)
29	The Gram-negative bacteria presence indicator	*N*-acyl homoserine lactones	MIP containing carbon QDs grafted on Fe_3O_4@SiO_2 magnetic NPs	Fluorescence	3.65×10^{-3}–0.96×10^{-1} μM	$2.98-6.27\times10^{-5}$ μM	–	Fish, juice, and milk	(Cui et al. 2020)
30	Pesticide	Indoxacarb	MIP film grafted on silica-carbon QDs	Fluorescence	4–102 nM	1 nM	–	Water, apple, and tomato	(Shirani et al. 2021)

(*Continued*)

Table 2. (Continued).

No.	Group of contaminants	Specific target	Details of MIP sensing protocol	Type of assay	Dynamic linear concentration range	LOD	Naked eye detection	Food product analyzed	Ref.
31	Dye	Tartrazine	MIP silica grafted on carbon QDs	Fluorescence	3.3–20.0 nM	1.3 nM	–	Saffron tea	(Zoughi et al. 2021)
32	Chemical contamination	di-*n*-Butyl phthalate	Zeolite imidazolate framework-67 microparticles were coated with CdTe QDs/imprinted silica composite	Fluorescence	50 nM–18 µM	1.6 nM	–	Water, fish, milk, juice	(Chen, Fu, et al. 2022)
33	Antibiotic	Thiamphenicol	CdTe*CdS*ZnS QDs and mesoporous carbon were embeds inside the imprinted silica particles	Fluorescence	0.1–100 µg L^{-1}	40 ng L^{-1}	Yes	Milk	(Sa-nguanprang, Phuruangrat, and Bunkoed 2022)
34	Chemical contamination	Phenanthrene	Magnetic Fe_3O_4 NPs and luminescent $LaVO_4$:Eu^{3+} NPs were embedded inside MIP particles	Luminescence	0–6 µg mL^{-1}	3.64 ng mL^{-1}.	Yes	Milk	(Li and Wang 2013)
35	Antibacterial agent	Enrofloxacin	MIP film was grafted by free-radical polymerization on the surface of upconverting NPs. The surface of these NPs was decorated with aptamers and template molecules before polymerization.	Luminescence	0.5–10 ng mL^{-1}	–	Yes	Perch, catfish, and Spanish mackerel	(Liu et al. 2017)
36	Chemical contamination	Melamine	The magnetic field-aligned photonic crystal of magnetic MIP particles	Colorimetric	10^{-5}–10^{-2} mg mL^{-1} [a]	1×10^{-5} mg mL^{-1}	Yes	–	(You, Cao, and Cao 2016)
37	Antibiotic	Chloramphenicol	The magnetic field-aligned photonic crystal of magnetic MIP particles	Colorimetric	10^{-3}–1.0 mg mL^{-1} [a]	1.0×10^{-3} mg mL^{-1}	Yes	–	(You et al. 2017)
38	Antibiotic	Tetracycline	Inverse opal MIP	Colorimetric	10^{-10}–10^{-6} M	–	–	Milk and meat	(Yang, Peng, et al. 2017)
39	Antibacterial agent	Sulfaguanidine	Inverse opal MIP	Colorimetric	10^{-8}–10^{-3} M [b]	2.8×10^{-10} M	–	Bass fish	(Li et al. 2019)
40	Illegal additive	Methyl anthranilate	Inverse opal MIP	Colorimetric	0.1–10 mM	31 µM	Yes	Wine	(Wu et al. 2019)
41	Mycotoxin	*α*-Amanitin	Inverse opal MIP	Colorimetric	10^{-9}–10^{-3} mg L^{-1}	5.0×10^{-10} mg L^{-1}	Yes	Mushroom	(Qiu et al. 2020)
42	Biogenic amines signaling food rottenness	Histamine	MIP film deposited via spin-coating on SPR chip	SPR	25–1000 ng mL^{-1}	25 ng mL^{-1}	–	Carp	(Jiang et al. 2015)
43	Antibiotic	Kanamycin	MIP film was polymerized on the activated SPR chip surface	SPR	1.0×10^{-7}–1.0×10^{-5} M	4.33×10^{-8} M	–	Milk powder	(Zhang et al. 2018)

44	Chemical contamination	Melamine	*o*-Aminophenol MIP film was deposited via electropolymerization on an optical fiber surface coated with Cr/Au film	SPR on optical fiber	10^{-10}–10^{-2} M [a]	5.1×10^{-12} M	–	–	(Li, Zheng, et al. 2018)
45	Allergen	*α*-Casein	250–450 nm MIP nanoparticles monolayer immobilized on SPR chip surface	SPR	0.5–8 ppm	0.127 ppm	–	Wash samples from cleaning-in-place systems	(Ashley et al. 2018)
46	Hormone	Ractopamine	Composite of MIP NPs, rGO, and Au NPs spin-coated on SPR chip surface	SPR	20–1000 ng mL^{-1}	5 ng/mL	–	–	(Yao et al. 2016)
47	Antibiotic	Vancomycin	175 nm MIP NPs monolayer was immobilized on the SPR chip surface; vancomycin was coupled with Au NPs to enhance the SPR signal	SPR	10–1000 ng mL^{-1}	4.1 ng mL^{-1}	–	Skimmed milk	(Altintas 2018)
48	Pesticide	Chlorpyrifos	Fe_3O_4@polydopamine MIP NPs were applied for analyte extraction and signal enhancement of AChE based SPR sensor	SPR	0.001–10 μM	0.76 nM	–	Apple	(Yao et al. 2013)
49	Mycotoxin	Patulin	Patulin imprinted NPs were emulsion polymerization method, and then they were drop-cast on SPR chip surface	SPR	500 pM–750 nM	11 pM	–	Apple juice	(Çimen, Bereli, and Denizli 2022)
50	Wine astringency	Saliva proteins	Glass slides, 100-nm in diameter Au disks of 20 nm thickness, and a 2-nm thick Ti underlayer were fabricated. Then saliva proteins were immobilized on Au nanodisks surface, and finally, MIP film was deposited	LSPR	1 to 140 μM expressed in PGG units [b]	–	–	Wine	(Guerreiro et al. 2017)

[a]Non-linear response.
[b]Linear in a semi-log scale.

Table 3. Examples of MIPs application for non-optical sensing in food samples.

No.	Group of contaminants	Specific targets	Details of MIP sensing protocol	Assay type	Dynamic linear concentration range	LOD	Food product analyzed	Ref.
Electrochemical sensors								
1	Heavy metal ions	Hg^{2+}	4-(2-Thiazolylazo) resorcinol was used as a functional monomer for free-radical MIP polymerization. The resulting MIP was homogenized into a paste with graphite powder, GO, and a 1-butyl-1-methylpyrrolidinium bis(trifluoromethylsulfonyl)imide ionic liquid	Potentiometry	4.00×10^{-9}–1.30×10^{-3} M[a]	1.95×10^{-9} M	Tuna and shrimp	(Shirzadmehr, Afkhami, and Madrakian 2015)
2	Pesticide	Lindane	MIP was grafted on the MWCNT surface via free-radical polymerization. MWCNT@MIP particles were dop-cast on Cu electrode and immobilized with polyagarose	Potentiometry	1.0×10^{-10}–1.0×10^{-5} M and 1.0×10^{-5}–1.0×10^{-3} M[a]	1.0×10^{-10} M	Grape, orange, tomato and cabbage	(Anirudhan and Alexander 2015)
3	Antibiotic	Neomycin	Polypyrrole MIP film was electropolymerized on the Au electrode modified with chitosan/Ag NPS/graphene/MWCNTs composite	Chronoamperometry	9.0×10^{-9}–7.0×10^{-6} M	7.63×10^{-9} M	Milk and honey	(Lian et al. 2013)
4	Antibiotic	Sulfadimethoxine	Polypyrrole MIP film was electropolymerized on the Au disk electrode	Chronoamperometry	0.17–1.1 mM and 1.3–3.7 mM	70 µM	Milk	(Turco, Corvaglia, and Mazzotta 2015)
5	Antibiotic	Sulfamethoxazole	Polydopamine MIP film was electropolymerized on an Au electrode	Chronoamperometry	0.8–170 µM	800 nM	Milk	(Turco et al. 2018)
6	Pesticide	Carbofuran	*o*-Phenylenediamine MIP was electropolymerized in the presence of 4-*tert*-butylcalix [8]arene on GCE decorated with MWCNTs and Fe_3O_4@Au NPs	Chronoamperometry in flow-injection analysis	0.1 to 100 µM	3.8 nM	Cabbage, celery, chili, onion, and peppermint	(Amatatongchai et al. 2018)
7	Flavor	Eugenol	MIP consisting of *p*-aminothiophenol and *p*-aminobenzoic acid as functional monomers were electropolymerized on the GCE modified with graphene/carbon nanotubes/1-aminopropy l-3-methylimidazolium bromide ionic liquid composite	Linear sweep voltammetry	5.0×10^{-7}–2.0×10^{-5} M	1.0×10^{-7} M	Curry	(Yang, Zhao, and Zeng 2016)
8	Insecticide	Imidacloprid	MIP was grafted on the GCE electrode surface decorated with graphene-modified with *p*-Vinylbenzoic acid via free-radical polymerization	Linear sweep voltammetry	0.5–15 µM Two linear responses (0.5–4.0 µM and 4.0–15 µM)	0.10 µM	Rice	(Zhang et al. 2017)
9	Chemical contamination	Bisphenol A	Imprinted chitosan/GO composite was drop-cast on acetylene black paste electrode surface	Second-order derivative linear sweep voltammetry	8.0 nM–1.0 µM and 1.0–20 µM	6 nM	Plastic bottled drinking water and canned beverages	(Deng, Xu, and Kuang 2014)

10	Antiprotozoal agent	Metronidazole	*o*-Phenylenediamine MIP film was electropolymerized on GCE coated with nanoporous nickel	Cyclic voltammetry	6×10^{-14}–4×10^{-13} M and 4.0×10^{-13}–4×10^{-12} M	2×10^{-14} M	Fish	(Li, Liu, et al. 2015)
11	Biogenic amines signaling food rottenness	Histamine	Magnetic Fe_3O_4/SiO_2/MIP NPs were synthesized by free-radical polymerization. They were collected on magnetic graphite-epoxy composite by magnetic field after analyte binding	Cyclic voltammetry	0–2.2×10^{4} mg L^{-1} and 0–11.1 mg L^{-1} with preconcentration of histamine[b]	1.6×10^{-6}mg L^{-1}	Fish	(Hassan et al. 2019)
12	Pesticide	Dimethoate	Polypirol MIP was electropolymerized on GCE	Square wave voltammetry	0.1–1 nM	0.5 nM	Wheat flour	(Capoferri et al. 2017)
13	Necessary nutrients	Caffeine	Silica MIP film was deposited on GCE decorated with MWCNTs by a sol-gel polymerization process	Differential pulse voltammetry	0.75–40 µM	0.22 µM	Coffee, instant coffee, and energy drink	(Santos et al. 2012)
14	Necessary nutrients	Quercetin	Polypyrrole MIP was electropolymerized on the surface of CGE modified with GO	Differential pulse voltammetry	6.0×10^{-7}–1.5×10^{-5} M[b]	4.8×10^{-8} M	Apple juice	(Sun et al. 2013)
15	Antibiotic	Erythromycin	MIP particles were synthesized via free-radical polymerization and then added to a carbon paste	Differential pulse voltammetry	5.0×10^{-8}–1.0×10^{-5} M	1.9×10^{-8} M	Honey	(Song et al. 2014)
16	Mycotoxin	T-2 toxin	Imprinted silica was deposited on GCE via electrochemically initiated polymerization. Fe^{3+} metal coordination was involved in analyte binding into the MIP cavity	Differential pulse voltammetry	1.12 nM–2.12 mM	0.33 nM	Corn, rice, and soybean	(Gao, Cao, et al. 2014)
17	Mycotoxin	Ochratoxin A	Polypyrrole MIP film electropolymerized on the surface of GCE decorated with MWCNTs	Differential pulse voltammetry	0.050–1 µM	4.1 nM	Beer, white and red wine	(Pacheco et al. 2015)
18	Chemical contamination	Tetrabromo-bisphenol A	Polypyrrole film was electropolymerized on the surface of a carbon electrode decorated with graphene and carbon nanotubes	Differential pulse voltammetry	1.0×10^{-11}–1.0×10^{-8} M[a]	3.7 pM	Catfish, chub, and carp	(Zhang et al. 2015)
19	Antibiotic	Dimetridazole	MIP was grafted on the Au NPs' surface by free-radical polymerization. Then it was mixed with mesoporous carbon and porous graphene. Finally, it was drop-cast on the GCE surface	Differential pulse voltammetry	2.0×10^{-9}–2.5×10^{-7} M and 2.5×10^{-7}–3.0×10^{-6} M	5×10^{-10} M	Milk, honey, and pork	(Yang and Zhao 2015)
20	Preservative	Propyl gallate	Silica MIP film was deposited with electrochemically initiated sol-gel polymerization on the surface of GCE decorated with graphene/SWCNTs	Differential pulse voltammetry	8.0×10^{-8}–2.6×10^{-3} M	5.0×10^{-8} M	Edible oil and instant noodle	(Xu et al. 2015)
21	Insecticide	Imidacloprid	Imprinted *o*-aminophenol was electropolymerized in the presence of 4-*tert*-butylcalix[6]arene and bromophenol blue catalysis on GCE decorated with Pt-In nanocomposite	Differential pulse voltammetry	2.0×10^{-10}–5.0×10^{-8} M	1.2×10^{-11} M	Tomato, cabbage, chili, and lettuce	(Li, Liu, et al. 2016)

(*Continued*)

Table 3. (Continued).

No.	Group of contaminants	Specific targets	Details of MIP sensing protocol	Assay type	Dynamic linear concentration range	LOD	Food product analyzed	Ref.
22	Food dye	Sunset yellow	MIP was grafted on the surface of magnetic GO/ Fe_3O_4/β-CD/1-butyl-3-methyl-imidazolium bromide ionic liquid/ Au NPs composite particles vie free-radical precipitation polymerization method. Then MIP composite particles were drop-cast on the GCE surface	Differential pulse voltammetry	1.0×10^{-8}–1.0×10^{-4} M	2 nM	Water and soft drinks	(Li, Wang, et al. 2016)
23	Chemical contamination	Bisphenol A	The GCE was modified with amino-functionalized graphene oxide. The amino groups were used to immobilize the template molecules on the graphene oxide surface. Finally, the MIP film was grafted by free-radical polymerization	Differential pulse voltammetry	6–100 nM and 0.2–20 µM	3 nM	Milk and mineralized water	(Dadkhah et al. 2016)
24	Hormone	17-β-Estradiol	MIP particles were synthesized by emulsion photopolymerization. Then, they were drop-cast on a carbon screen-printed electrode decorated with MWCNTS and Au NPs	Differential pulse voltammetry	1.0×10^{-15}–1.0×10^{-6} M[a]	2.5×10^{-16} M	Arowana fish	(Futra et al. 2016)
25	Mycotoxin	Patulin	*p*-Aminothiophenol MIP film was electropolymerized on GCE decorated with carbon QDs and Au NPs	Differential pulse voltammetry	1×10^{-12} to 1×10^{-9} M[a]	7.57×10^{-13} M	Apple juice	(Guo et al. 2017)
26	Synthetic hormone	Diethylstilbestrol	The imprinted silica was deposited using an electrochemically initiated sol-gel process on GCE modified with Au NPs, MWCNTs, and chitosan composite	Differential pulse voltammetry	1.0×10^{-10}–1.0×10^{-6}mg mL^{-1} [a]	24.3 fg mL^{-1}	Milk	(Bai et al. 2017)
27	Grow factor	Salbutamol	*o*-Phenylenediamine MIP was electropolymerized on GCE decorated with Ag/*N*-doped rGO composite	Differential pulse voltammetry	0.03–20.00 µM	7 nM	Pork	(Li, Xu, et al. 2017)
28	Insecticides	Methamidophos Omethoate	Silica MIP was grafted on MOF NP's surface via a sol-gel polymerization method. Then, Fe_3O_4@rGO NPs and MOF@MIP NPs were drop-cast on the GCE surface	Differential pulse voltammetry	1.0×10^{-7}–1.0×10^{-12} M[a] 1.0×10^{-7}–1.0×10^{-13} M[a]	2.67×10^{-13} M 2.05×10^{-14} M	Cucumber and kidney bean	(Shi et al. 2017)
29	Necessary nutrients	Quercetin	Imprinted poly(*p*-aminobenzoic acid) was electropolymerized over the GCE surface decorated with Pd NPs, porous graphene, and carbon nanotubes	Differential pulse voltammetry	10–500 nM	5 nM	Honeysuckle juice and red wine	(Yang, Xu, et al. 2017)
30	Preservative	*tert*-Butylhydroquinone	Polyphenol MIP was deposited by electropolymerization over GCE decorated with Ag@($H_3PW_{12}O_{40}$ polyoxometalate)@rGO particles	Differential pulse voltammetry	0.05–1.5 nM	14.8 pM	Soybean oil, blend oil, and beef tallow	(Qin et al. 2017)

31	Flavor	Vanillin	MIP film was grafted on the surface of MWCNTs@polydopamine NPs with free-radical polymerization using 1-vinyl-3-octylimidazole hexafluoride phosphorus as a functional monomer. MWCNTs@polydopamine@MIP particles were drop-cast on the GCE decorated with SWCNTs	Differential pulse voltammetry	0.2–10 μM	0.1 μM	Biscuit, cake, and milk tea	(Wu, Yang, et al. 2017)
32	Antibiotic	Olaquindox	Phenylenediamine MIP film was electropolymerized, and the surface of GCE was decorated with MWCNTs and Au NPs	Differential pulse voltammetry	10–200 nM	2.7 nM	Pork and fish	(Wang, Yao, et al. 2017)
33	Dye	Sunset yellow	Polydopamine MIP was grafted on MWCNTs via a self-polymerization process. Then, MWCNTs@MIP NPs were drop-cast on GCE	Differential pulse voltammetry	2.2 nM–4.64 μM	1.4 nM	Jelly, fruit drink, chocolate, instant juice powder, ice cream, and candy	(Yin, Cheng, et al. 2018)
34	Fungicide	Tebuconazole	Imprinted *o*-aminophenol and resorcinol as functional monomer copolymer film was electropolymerized over GCE decorated with AuNPs, thiolated graphene, and (Prussian blue)@Au NPs	Differential pulse voltammetry	5.0×10^{-8}–4.0×10^{-4} M[a]	1.25×10^{-8} M	Cucumber, green vegetables, and strawberry	(Qi et al. 2018)
35	Antibiotic	Sulfonamide	MIP NPs were synthesized by free-radical polymerization. Then, they were immobilized on a Ni nanofoam electrode decorated with NiO_2 NPs	Differential pulse voltammetry	5.9×10^{-7}–1.34×10^{-3} M	3.57×10^{-7} M	Fish	(Liu et al. 2019)
36	Chemical contamination	Melamine	(Acrylic acid)/ethylhexyl acrylate/7-(4-vinylbenzyloxy)-4-methyl coumarin copolymer was synthesized by free radical polymerization. Then, it was mixed with the temple (melamine) and MWCNTs, drop-cast on GCE, and cross-linked via UV light-induced polymerization of coumarin moieties	Differential pulse stripping voltammetry	1.0×10^{-12}–1.0×10^{-6} M[a]	5.6×10^{-13} M	Milk	(Xu et al. 2018)
37	Hazardous dietary supplement	*p*-Synephrine	MIP film was electropolymerized with (*bis*-bithiophene)-based functional monomers containing carboxylic acid and ferrocene moieties	Differential pulse voltammetry with self-reporting MIP film	0.2–8.8 nM	0.57 nM	Dietary supplement for body-builders	(Lach et al. 2021)
38	Carcinogen	*N*-Nitroso-L-proline	MIP film was electropolymerized with (*bis*-bithiophene)-based functional monomers containing phenol moieties	Differential pulse voltammetry	9.1–43.9 μM	80.9 nM	Grilled pork neck	(Lach et al. 2017)
				EIS	9.1–43.9 μM	36.9 nM	–	
				E-QCM	0.125 – 2.0 mM	10 μM	–	

(*Continued*)

Table 3. (Continued).

No.	Group of contaminants	Specific targets	Details of MIP sensing protocol	Assay type	Dynamic linear concentration range	LOD	Food product analyzed	Ref.
39	Hazardous dietary supplement	*p*-Synephrine	MIP film was electropolymerized with (*bis*-bithiophene)-based functional monomers containing carboxylic acid moieties	Differential pulse voltammetry	0.1–0.99 µM	12.2 nM	–	(Lach et al. 2019)
				EIS	0.1–0.99 µM	5.69 nM	–	
				SPR	0.45–2.06 mM	6.9 µM	–	
40	Biogenic amines signaling food rottenness	Tyramine	MIP film was electropolymerized with (*bis*-bithiophene)-based functional monomers containing crown ether and carboxylic acid moieties	Differential pulse voltammetry	290 µM–2.64 mM	159 µM	Mozzarella cheese whey	(Ayerdurai, Cieplak, et al. 2021)
				EIS	290 µM–2.64 mM	168 µM	–	
41	Mycotoxin	Fumonisin B1	MIP NPs were synthesized via free-radical polymerization and then covalently immobilized on Pt electrode coated with polypyrrole/ Zink porphyrin conductive composite film	Differential pulse voltammetry	1 fM–10 pM[a]	0.03 fM	Maise	(Munawar et al. 2020)
				EIS	1 fM–10 pM[a]	0.7 fM	–	
42	Chemical contamination	Melamine	GCE was decorated with rGO and conditioned in 1% H_2O_2 solution in alkaline water/acetonitrile mixt solvent. Then, MIP polypyrrole film electropolymerized on the electrode surface.	EIS	4.0–240 nM	0.83 nM	Milk	(Shamsipur, Moradi, and Pashabadi 2018)
43	Carcinogen	2-Amino-3,7,8-trimethyl-3*H*-imidazo[4,5-*f*] quinoxaline	MIP film was electropolymerized with (*bis*-bithiophene)-based functional monomers containing adenine and one thymine moieties	Capacitive impedimetry	47–400 µM	15.5 µM	Pork meat	(Ayerdurai, Garcia-Cruz, et al. 2021)
Electrochemiluminescence sensors								
44	Antibiotic	Lincomycin	*o*-Aminophenol MIP film was electropolymerized in the presence of lincomycin and carbon QD-labeled aptamer on Au NPs and GO decorated GCE	ECL	5.0×10^{-12}–1.0×10^{-9} M	1.6×10^{-13} M	Chicken, duck, crucian, pork, crab, beef, and mutton	(Li, Liu, et al. 2017)
45	Hazardous dietary supplement	Clenbuterol	*o*-Phenylenediamine MIP film was electropolymerized on GCE decorated with rGO and upconverting $NaYF_4$:Yb, Er NPs	ECL	10 nM–100 µM	6.3 nM	Pork meat, liver, and kidney	(Jin et al. 2018)
46	Antibiotic	Enrofloxacin	*o*-Phenylenediamine MIP film was electropolymerized on an electrode surface decorated with mercaptopropionic acid-functionalized Cu nanoclusters	ECL	100 pM–1 µM	27 pM	Beef, pork, pork liver, and fish	(Wang et al. 2022)
47	Illegal fertilizer	Clenbuterol	Polypyrrole MIP film was electropolymerized on a GCE surface decorated with Fe_2O_3 microfibers decorated with $Ru(bpy)_3^{2+}$	ECL	1 nM–100 µM	330 pM	Pork and liver	(Zhao et al. 2022)
48	Herbicide	Prometryn	*o*-Aminophenol MIP film was electropolymerized on an electrode surface decorated with $CsPbBr_3$ perovskite QDs	ECL	0.1–500 µg L^{-1}	50 ng L^{-1}	Fish	(Zhang et al. 2022)

Piezoelectric microgravimetry								
49	Chemical contamination	Melamine	MIP film was electropolymerized with (*bis*-bithiophene)-based functional monomers containing crown ether moieties	E-QCM (flow analysis)	5 nM–1 mM	5 nM	Kefir	(Pietrzyk et al. 2009)
50	*Staphylococcus aureus* pathogenic bacteria	Staphylococcal enterotoxin A	Silica MIP was deposited on QCR by spin-coating	QCM	0.1–1000 µg mL^{-1}[b]	7.97 ng mL^{-1}	Milk	(Liu et al. 2014)
		Staphylococcal enterotoxin B			0.1–1000 µg mL^{-1}[b]	2.25 ng mL^{-1}		
51	Antibiotic	Chloramphenicol	MIP synthesized by free-radical precipitation polymerization was embedded into PVC membrane deposited on QCR by spin-coating	QCM	1.0×10^{-6}–1.0×10^{-1} µg mL^{-1} [a]	7×10^{-8} µg mL^{-1}	Pork, honey, milk, and prawn	(Ebarvia, Ubando, and Sevilla 2015)
52	Pesticide	Metolcarb	MIP synthesized by free-radical polymerization was grounded and embedded into PVC membrane deposited on QCR	QCM	5–70 µg L^{-1}	2.3 µg L^{-1}	Apple juice, pear, and cabbage	(Fang et al. 2017)
53	Pesticide	Methyl parathion	Solution of poly(vinylidene fluoride) and template was drop-cast on QCR surface	QCM (flow analysis)	1–87 µM	68 nM	Vegetable cos lettuce	(Lin et al. 2018)
54	Pesticide	Trichlorfon	Poly(vinylidene fluoride) was treated with alkali conditions in the presence of a template and then drop-cast on the QCR surface	QCM	0–250 ppb	4.63 ppb	Iceberg lettuce	(Dayal et al. 2019)
55	Antithyroid drug	Methimazole	MIP was grafted on hollow silica spheres' surface by free-radical polymerization and was embedded into PVC membrane drop-cast on QCR	QCM	5–70 µg L^{-1}	3 µg L^{-1}	Pork, beef, and milk	(Zhao, He, et al. 2020)
56	Chemical contamination	Melamine	MIP was grafted on allylmercaptan decorated Au surface of QCR via free-radical polymerization	QCM	1–10 µg L^{-1} and 50–1000 µg L^{-1}	2.3 µg L^{-1}	Milk	(Ceylan Cömert et al. 2022)
Field-effect transistors								
57	Allergen	Gluten epitope	MIP film was electropolymerized with (*bis*-bithiophene)-based functional monomers containing benzoic acid and cytosine moieties	EG-FET	0.5–45 ppm[a]	0.11 ppm	Semolina flour	(Iskierko et al. 2019)
Thermal sensors								
58	Antibiotic	Nitrofurantoin	MIP synthesized by free-radical polymerization was grounded and packed in a 500 µL microreactor connected with the thermistor probe	Flow-through thermometric calorimeter	5–50 µM	–	Poultry feed	(Athikomrattanakul, Gajovic-Eichelmann, and Scheller 2011)
59	Bacteria	*E. coli*	MIP was synthesized by cross-linking bisphenol A (functional monomer) with a phloroglucinol cross-linker and then was spin-coated on a stainless-steel thermistor surface. Finally, bacteria coated stamp was pressed and left to cure for 18 h at 65 °C	Heat-transfer method using specially designed microfluidic chip	1 k–10 k CFU mL^{-1}	100 CFU mL^{-1}	Apple juice	(Cornelis et al. 2019)

(*Continued*)

Table 3. (Continued).

No.	Group of contaminants	Specific targets	Details of MIP sensing protocol	Assay type	Dynamic linear concentration range	LOD	Food product analyzed	Ref.
Miscellaneous								
60	Hormone	17β-Estradiol	Imprinted silica was grafted on a paper surface	MIP grafted paper was applied as a solid substrate for a competitive ELISA-like assay using 17β-Estradiol-labeled HRP	Naked-eye detection[b]	0.25 µg L^{-1}	Milk	(Xiao et al. 2017)
61	Mycotoxin	Patulin	Ag NPs were synthesized inside of the Zn-based flake like MOF. Then imprinted silica film was grafted on the surface of AgNPs@MOF nanocomposite	AgNPs@MOF@MIP nanocomposite catalyzed terephthalic acid oxidation in the presence of H_2O_2. Highly fluorescent 2-hydroxyterephthalic acid was formed. Patulin binding into MIP inhibited this reaction	0.1–10 µM	0.06 µM	Apple juice	(Bagheri et al. 2018)
62	Insecticide	Carbofuran	MIP particles were synthesized by free-radical polymerization	MIP particles were introduced in the microfluidic chip to separate and pre-concentrate the analyte in the samples. The analyte was determined with differential pulse voltammetry on the Au electrode decorated with GO@Au NPs and carbofuran targeted DNA aptamer. The electrode was located in another compartment of the microfluidic chip	0.2–50 nM	67 pM	Chinese cabbage, chili, lettuce, tomato, apple, banana, tangerine, and watermelon	(Li, Li, et al. 2018)

[a]Linear in a semi-log scale.
[b]Non-linear response.

Fluorescence transduction application results in assays of enhanced sensitivity. Accordingly, a competitive fluorescent assay for histamine in the fish extract was reported (Mattsson et al. 2018). MIP particles and a fluorescence-tagged histamine derivative were added to the sample solutions examined. Then, the histamine content in the solution was indirectly determined by evaluating the amount of fluorescent derivative remaining in the solution after mixing with MIP particles. In another report, a catalytically active AgNPs@MOF@MIP (where MOF denotes a metal-organic framework) nanocomposite was proposed (Bagheri et al. 2018). In the H_2O_2 presence, terephthalic acid oxidation to fluorescent 2-hydroxyterephthalic acid was catalyzed. The patulin analyte inhibited this reaction by binding to MIP cavities, thus lowering the recorded fluorescence intensity. Moreover, a very fast and robust ELISA-like competitive assay was devised by depositing 17β-estradiol imprinted silica on the surface of a filter paper chemosensor (Scheme 4c) (Xiao et al. 2017). The target analyte competition with estradiol-labeled horseradish peroxidase (HRP) allowed for naked-eye 17β-estradiol detection by soaking the sensor in a solution of a colored reaction substrate. For milk samples containing 17β-estradiol, the color change was much less pronounced.

The above procedures require using costly and environmentally unfriendly chemicals. Moreover, most of these chemicals are being dumped into waste after use. Therefore, they are cost-ineffective and non-ecological. It is much more reasonable to synthesize MIP particles to serve as dyes themselves (Scheme 4a, I). Toward that, MIP particles containing co-polymerized fluorescent monomers were synthesized (Gao, Li, et al. 2014; Ashley, Feng, and Sun 2018; Li, Yin, et al. 2015). Moreover, an MIP film can be grafted on the surface of fluorescent quantum dots (QDs) (Sun et al. 2018; Wang, Fang, et al. 2017; Jalili et al. 2020; Wu, Lin, et al. 2017; Li, Jiao, et al. 2018; Fang et al. 2019; Cui et al. 2020; Shirani et al. 2021; Zoughi et al. 2021; Chen, Fu, et al. 2022; Sa-nguanprang, Phuruangrat, and Bunkoed 2022) or luminescent upconverting NPs (Liu et al. 2017). Those particles can be collected and regenerated after the assay and re-used many times. Recently, dual-emission MIP fluorescent particles were invented (Jalili et al. 2020). They were synthesized in two steps in a one-pot reaction. First, silica core particles containing (blue light)-emitting carbon QDs were synthesized. Then, a penicillin G imprinted mesoporous silica film containing (yellow light)-emitting carbon QDs was grafted as a shell. Due to spatial separation of (blue light)-emitting QDs, the penicillin G analyte binding in imprinted molecular cavities quenched the fluorescence of only (yellow light)-emitting carbon QDs. As tested on milk samples, a pronounced color change in the penicillin G analyte presence was observed even with the naked eye. In another report, using the sonication encapsulation method, luminescent and magnetic NPs were entrapped in MIP nanocomposites (Li and Wang 2013). Magnetic field-driven MIP nanocomposites separation from the sample solution decreased interference from other polycyclic aromatic hydrocarbons (PAHs), and only the phenanthrene target analyte significantly quenched the MIP luminescence. MIP nanocomposites emitted red light ($\lambda = 620$ nm). Therefore, the naked eye readily observed luminescence intensity changes due to phenanthrene presence.

Another procedure involved devising label-free optical assays. For that, MIPs were deposited on the surface of gold-layered SPR chips as thin films (Scheme 6a, I and V) (Jiang et al. 2015; Zhang et al. 2018), or MIP NPs' monolayers (Ashley et al. 2018; Yao et al. 2016; Çimen, Bereli, and Denizli 2022). In this case, analyte binding in MIP caused a change in the electric permittivity of the film that was in contact with an ultra-thin gold film deposited on the SPR chip surface. This binding shifts the evanescing light angle and wavelength, at which resonance with surface plasmon occurs. Thus, light is being absorbed. However, this approach is usually dedicated to determining macromolecular compounds, and SPR determination sensitivity to small-molecule compounds is relatively low. Therefore, Au NPs (Altintas 2018) and magnetic MIP NPs (Yao et al. 2013) were applied to enhance the sensitivity of SPR chemosensors. Moreover, the SPR spectrometer readout depends on the angle of the light evanescence. It makes chemosensors susceptible to mechanical vibrations and thus useless for in-field assays. Therefore, an MIP film was deposited by electropolymerization on the surface of an optical fiber to overcome this deficiency (Li, Zheng, et al. 2018). To this end, fibers were unclothed using a sharp blade, and then the cladding of sensing sections was entirely removed by immersing them in an HF solution. Finally, a 5-nm thick Cr underlayer and a 50-nm thick Au layer were consecutively sputtered on the sensing section of the optical fiber sensor. This Au layer served as the working electrode during deposition by electropolymerization of the MIP film, and a transducer sensitive to analyte binding to the MIP imprinted cavities. In another example, an MIP film was deposited on a 100-nm diameter Au nanodisks array (Guerreiro et al. 2017). Thus, changes in localized surface plasmon resonance were monitored.

Very robust label-free optical chemosensors based on MIP photonic structures were proposed. To this end, a magnetic field-assisted colloidal crystal of magnetic MIP NPs was deposited (Scheme 4d) (You, Cao, and Cao 2016; You et al. 2017). In another approach, MIP films of the inverse opal structures were synthesized using silica beads as sacrificial molds (Scheme 4e) (Yang, Peng, et al. 2017; Li et al. 2019; Wu et al. 2019; Qiu et al. 2020). In both cases, analyte binding in the MIP film caused this film to swell and or to change its electric permittivity. In turn, that generated a significant change in the film color originating from Bragg diffraction. That way, toxins in various food samples were determined. The MIP chemosensors based on the colloidal crystals or the inverse-opal structures seem promising candidates for hand-held portable device fabrication applications. That is because of their robustness, independence from any external power supplies, and the possibility to detect analytes just by naked eye observation of the color change.

Furthermore, surface-enhanced Raman spectroscopy (SERS) transduction was combined with MIP recognition. The advantages of SERS sensors, including high sensitivity and qualitative analyte identification, were improved by MIPs

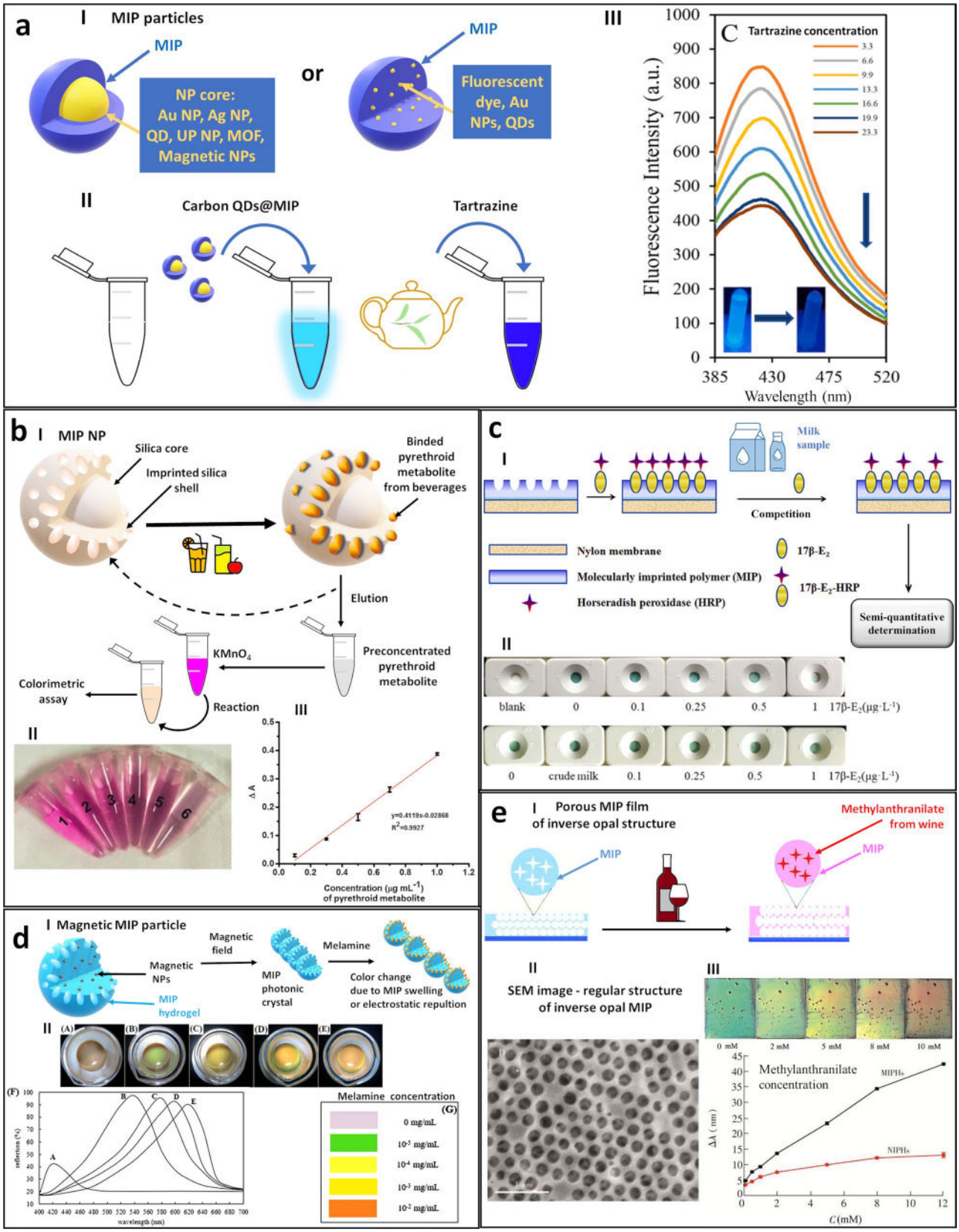

Scheme 4. (a I) A typical structure of MIP nanoparticles synthesized for optical assays. (a II and a III) An example of a fluorescent MIP optical assay. Carbon QD@MIP core-shell fluorescent NPs applied for tartrazine determination in saffron tea. Adapted from Zoughi et al. (2021); (b) Colorimetric determination of pyrethroid metabolite in fruit juice and beverages based on adsorption-desorption on imprinted silica NPs and color reaction with $KMnO_4$, adapted from Ye et al. (2018). A competitive assay for naked-eye semi-quantitative determination of 17β-E_2 hormone in milk using MIP-coated nylon membrane and horseradish peroxidase (HRP) labeled 17β-E_2, adapted from Xiao et al. (2017); (d) Photonic structures of magnetic MIP particles assembled in a magnetic field applied for colorimetric determination of melamine, adapted from You, Cao, and Cao (2016); (e) Color changes of inverse-opal MIP film to methyl anthranilate concentration changes allow semi-quantitative detection of the target analyte in wine samples, adapted from Wu et al. (2019).

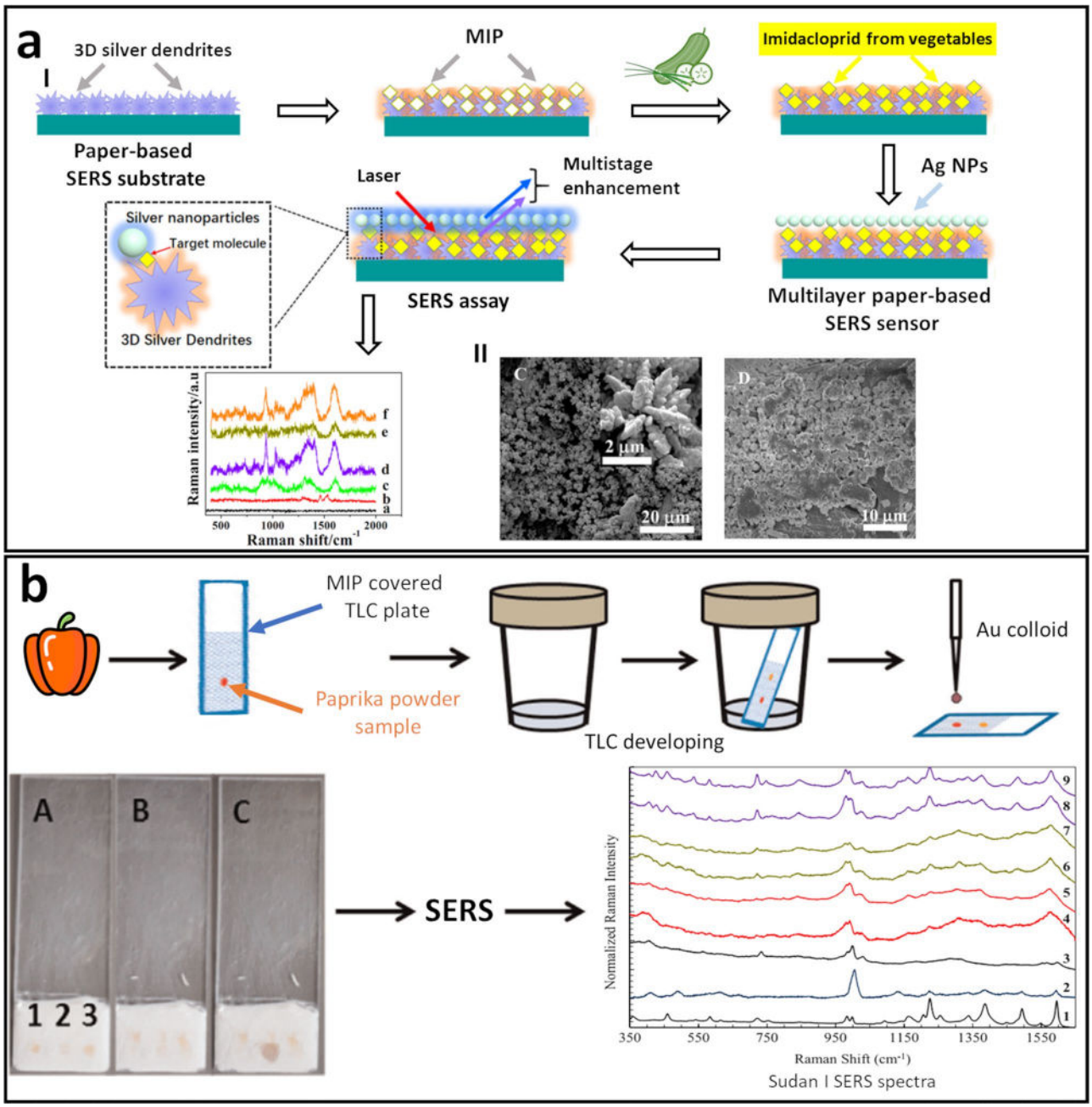

Scheme 5. (a) Multilayer paper SERS chemosensor based on star-shaped silver dendrites, MIP film, and Ag NPs for imidacloprid determination in the cucumber, chives, and soybean samples. Adapted from Zhao, Liu, et al. (2020); (b) Combining TLC on the MIP film-coated plate with SERS assay for selective Sudan I determination in the paprika extract samples. Adapted from Gao et al. (2015).

selectivity. MIPs were applied for sample pretreatment in the most robust approach before the SERS assay to pre-concentrate and purify the target analyte (Feng et al. 2017; Feng et al. 2013; Wu et al. 2016; Hua et al. 2018; Feng et al. 2018; Zhao et al. 2019). Moreover, an Au NPs suspension was applied for extraction to collect the analyte, namely, histamine, accumulated on the MIP SPE column (Gao, Grant, and Lu 2015). In more advanced procedures, the bulk MIPs were decorated with Au (Xie et al. 2017; Wang et al. 2020) and Ag (Hu and Lu 2016) NPs. Alternately, a thin MIP film was grafted on the surface of Au NPs (Zhou et al. 2020; Yin, Wu, et al. 2018) or ZnO@TiO_2@Ag NPs (Chen, Wang, et al. 2022). Similarly, a filter paper was coated with carbon ink on one side and decorated with silver dendrites on the other (Scheme 5a) (Zhao, Liu, et al. 2020). Then, an MIP was deposited by electropolymerization inside this paper. Ag NPs were synthesized on top of the MIP to enhance the SERS signal. In these procedures, analyte extraction and SERS determination were performed simultaneously. Various vegetable samples were tested in this manner. In another report, MIP microparticles served as a thin-layer chromatography (TLC) stationary phase (Gao et al. 2015). After developing and drying, the TLC plate was decorated with Au NPs, and the SERS signal was recorded (Scheme 5b). That enabled rapid Sudan I determination in paprika powder with minimal sample pretreatment.

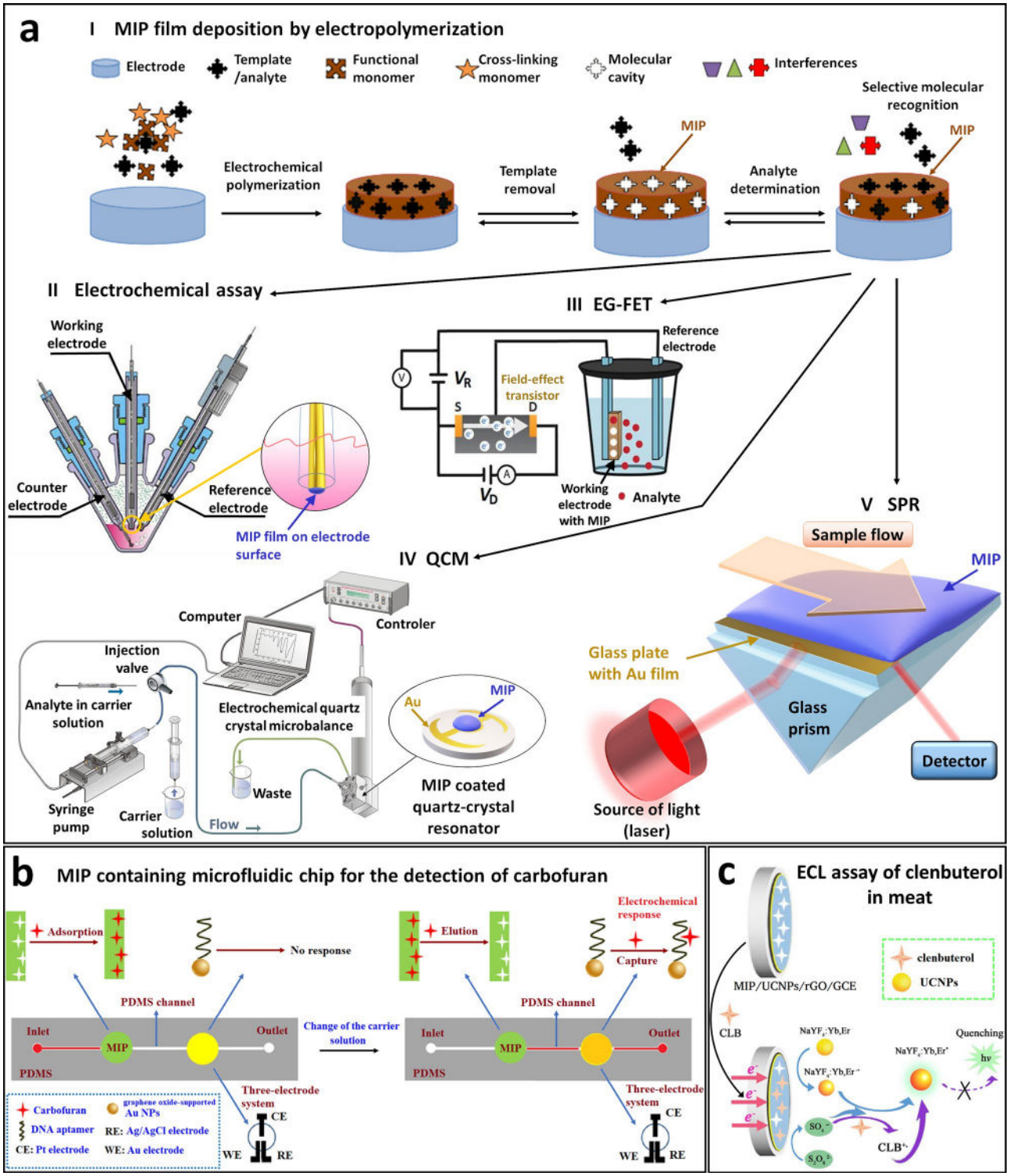

Scheme 6. (a) Examples of the most common MIP chemosensors including (I) a general procedure of thin MIP film deposition on the sensors' surface. Simplified schemes of (II) electrochemical, (III) EG-FET, (IV) QCM, and (V) SPR MIP chemosensors, adapted respectively, from (I) (Sharma et al. 2012); (II) (Pieta et al. 2013); (III) (Iskierko et al. 2016), and (IV) (Dabrowski et al. 2016); (b) Microfluidic devise for simultaneous purification and electrochemical determination of carbofuran in fruit and vegetable samples. Adapted from Li, Li, et al. (2018); (c) ECL assay based on MIP film and upconverting NPs for clenbuterol determination in meat samples. Adapted from Jin et al. (2018).

4.2. Electrochemical MIP chemosensors

Electrochemical sensors are gaining more and more interest because of their robustness, easy operation, and highly reproducible determinations. However, they usually suffer from low selectivity. The biological receptor immobilization on the electrode surface enables circumventing this disadvantage. Despite high selectivity and sensitivity, prepared that way, electrochemical biosensors reveal many deficiencies, mainly originating from the fragility of the biological recognition units used for their fabrication. Therefore,

electrodes coated with selective MIP films (Scheme 6a, I and 6a, II) have recently attracted more and more interest. So far, numerous examples of MIP film-coated electrodes have been reported for possible application in food quality control. Charged compounds can easily be determined with potentiometry (Shirzadmehr, Afkhami, and Madrakian 2015; Anirudhan and Alexander 2015). This technique usually covers a broad concentration range. But, by its nature, the potentiometric sensor's response linearly depends on the logarithm of concentration. Hence, it is insensitive to small changes in the analyte concentration.

If the target analyte is electroactive, it can be determined by recording its oxidation or reduction current changes with time by chronoamperometry at a selected constant potential applied (Lian et al. 2013; Turco, Corvaglia, and Mazzotta 2015; Turco et al. 2018; Amatatongchai et al. 2018). But there is a substantial limitation. That is, the target analyte must be the only electroactive component of the sample in the studied potential range. Voltammetric techniques enable partial overcoming of this deficiency. However, the faradaic currents originating from electrode reactions are overlapped by interfering capacity currents in a simple representation (Yang, Zhao, and Zeng 2016; Zhang et al. 2017; Deng, Xu, and Kuang 2014; Hassan et al. 2019; Li, Liu, et al. 2015). These undesired currents are subtracted in advanced voltammetry techniques, e.g., differential pulse voltammetry (DPV). Therefore, DPV sensitivity is very high, and the limit of detection (LOD) is low (Liu et al. 2022). Importantly, these techniques are dedicated to determining electroactive analytes (Yang, Zhao, and Zeng 2016; Zhang et al. 2017; Deng, Xu, and Kuang 2014; Hassan et al. 2019; Li, Liu, et al. 2015). If the target analyte is electroinactive, MIP chemosensors can signify their advantage. Electroinactive analytes may be determined using the so-called "gate effect" (Sharma et al. 2019). For that, a redox probe is added to the sample solution, and changes in the faradaic current caused by the changes in MIP film properties incurred by analyte binding are recorded (Sharma et al. 2019). Interestingly, redox probes can also be immobilized inside the MIP film (Lach et al. 2021). Moreover, such advanced techniques as electrochemical impedance spectroscopy (EIS) not only provide insight into the mechanism of the electrode processes (Sharma et al. 2019) but may also serve as a sensitive transduction tool for analyte determination (Lach et al. 2017; Lach et al. 2019; Ayerdurai, Cieplak, et al. 2021; Munawar et al. 2020; Shamsipur, Moradi, and Pashabadi 2018). In another example, capacitive impedimetry at MIP film-coated electrode was applied to determine cancerogenic aromatic amines in meat samples (Ayerdurai, Garcia-Cruz, et al. 2021).

Electrochemical redox processes can be combined with optical transduction to enhance the sensitivity and selectivity of determinations involving MIPs. For that, quenching of electrochemiluminescence (ELC) resulting from analyte binding by an MIP was applied (Li, Liu, et al. 2017; Zhang et al. 2022; Wang et al. 2022; Zhao et al. 2022; Jin et al. 2018). MIP thin films were deposited by electropolymerization on the electrodes decorated with carbon QDs (Li, Liu, et al. 2017; Zhang et al. 2022), Cu nanoclusters (Wang et al. 2022), and $Ru(bpy)_3^{2+}$ decorated Fe_2O_3 microfibers (Zhao et al. 2022) or upconverting NPs (Jin et al. 2018; Scheme 6c). Au NPs, GO, and rGO were deposited on the electrodes to increase the electrode surface area and conductivity. Thus, reagents enabling electron transfer in their excited states were electrochemically generated on NPs more efficiently. Analyte molecules binding in MIP cavities disturb this process. Therefore, it was possible to determine target analytes at very low concentrations.

4.3. Other types of MIP chemosensors

Molecular imprinting was also combined with several other transduction techniques. For instance, MIP films were successfully deposited on the surface of quartz crystal resonators (Scheme 6a, IV) (Lach et al. 2017; Pietrzyk et al. 2009; Liu et al. 2014; Ebarvia, Ubando, and Sevilla 2015; Fang et al. 2017; Lin et al. 2018; Dayal et al. 2019; Zhao, He, et al. 2020; Ceylan Cömert et al. 2022). Then, the MIP film mass changes caused by analyte binding were measured by piezoelectric microgravimetry using a quartz crystal microbalance (QCM). This microgravimetry is a very sensitive technique enabling mass change measurements down to nanograms, i.e., below a monolayer coverage. However, QCM is very difficult to miniaturize into a hand-held device. On the contrary, sensors based on field-effect transistors (FETs), especially the extended-gate field-effect transistors (EG-FETs), seem to ease miniaturizing because of their robustness. Moreover, the high sensitivity and selectivity of EG-FET chemosensors make them attractive candidates for portable analytical devices useful for in-field measurements. For instance, rapid gluten determination in semolina flour was reported (Scheme 6a, III) (Iskierko et al. 2019).

Noteworthy, a microfluidic MIP-based device for carbofuran determination in fruit and vegetable samples was fabricated (Scheme 6b) (Li, Li, et al. 2018). This device consisted of two compartments connected with microchannels. One compartment contained the MIP that ensured sample purification and analyte preconcentration, while the other served as an electrochemical cell with a working electrode decorated with the DNA aptamer targeted to carbofuran. This aptamer ensured additional enhancement in both sensitivity and selectivity of the chemosensor. In another procedure, microfluidic chips containing microreactors connected to miniaturized thermistors were reported (Athikomrattanakul, Gajovic-Eichelmann, and Scheller 2011; Cornelis et al. 2019). These microreactors contained MIP NPs (Athikomrattanakul, Gajovic-Eichelmann, and Scheller 2011) or a surface imprinted MIP film (Cornelis et al. 2019). Then, the thermistors determined the heat released because of the strong interactions of the target analyte (Athikomrattanakul, Gajovic-Eichelmann, and Scheller 2011) or bacteria (Cornelis et al. 2019) with MIP molecular cavities.

5. Applications of MIP chemosensors in food products analysis

Although MIP-based chemosensors are still unavailable commercially, numerous possible applications in food product analysis were reported in the literature. The most evident applications include detecting and quantizing toxic contaminants in food products. Most of these contaminants originate from incorrect methods of plant cultivation and animal breeding. These contaminants include pesticides (Yao et al. 2013; Ye et al. 2018; Shirani et al. 2021; Amatatongchai et al. 2018; Capoferri et al. 2017; Fang et al. 2017; Lin et al. 2018; Dayal et al. 2019), insecticides (Wu et al. 2018; Feng et al. 2017; Zhao, Liu, et al. 2020; Zhang et al. 2017; Li, Liu, et al. 2016; Shi et al. 2017; Li, Li, et al. 2018), and herbicides (Zhao et al. 2019) in plants. In the case of meat products, mostly antibiotics (Tarannum, Khatoon, and Dzantiev 2020; Wang et al. 2022), hormones (Yao et al. 2016), fertilizers (J. H. Li, Xu, et al. 2017; Zhao et al. 2022), and introduced during high-temperature processing carcinogens (Lach et al. 2017; Ayerdurai, Garcia-Cruz, et al. 2021) are being determined. Fish products are even more at risk of harmful contamination than regular meat products. Accordingly, such toxins as heavy metal ions (Shirzadmehr, Afkhami, and Madrakian 2015), insecticides (Li, Jiao, et al. 2018), herbicides (Zhang et al. 2022), antibiotics (Liu et al. 2017; Li, Liu, et al. 2015; Wang, Yao, et al. 2017; Liu et al. 2019; Wang et al. 2022), bisphenols (Zhang et al. 2015), and hormones (Futra et al. 2016) were determined in fish using MIP-based chemosensors. Milk and honey, similarly to fish, belong to a group of food products of most concern. Therefore, numerous MIP sensors were devised to determine hormones (Bai et al. 2017; Xiao et al. 2017), herbicides (Hua et al. 2018), antibiotics (Xie et al. 2017; Yang, Peng, et al. 2017; Zhang et al. 2018; Altintas 2018; Lian et al. 2013; Turco, Corvaglia, and Mazzotta 2015; Turco et al. 2018; Yang and Zhao 2015; Ebarvia, Ubando, and Sevilla 2015; Sa-nguanprang, Phuruangrat, and Bunkoed 2022), and chemical contaminants (Li and Wang 2013; Zhao, He, et al. 2020; Chen, Fu, et al. 2022) including bisphenols (Yin, Wu, et al. 2018; Dadkhah et al. 2016) in milk. Similarly, MIP chemosensors for pesticides (Gao, Li, et al. 2014) and antibiotics (Lian et al. 2013; Song et al. 2014; Yang and Zhao 2015; Ebarvia, Ubando, and Sevilla 2015) determination in honey were proposed. All toxins mentioned above were introduced to food products unwittingly by producers. However, there are also examples of intentional contamination of food. This contamination is incurred because of food product falsification. In most cases, food products are being artificially colored. Therefore, several MIP chemosensors for dyes in fish (Wu, Lin, et al. 2017), tea (Zoughi et al. 2021), soft drinks (Li, Wang, et al. 2016; Wang et al. 2020; Yin, Cheng, et al. 2018), jelly (Yin, Cheng, et al. 2018), ice cream (Yin, Cheng, et al. 2018), and candy (Yin, Cheng, et al. 2018) were devised. Milk falsification is much more serious misconduct. That is, falsified milk products are purposefully contaminated with melamine (Li, Song, and Wen 2019). The reason is a false increase in detected protein levels in low-quality milk products. Consumption of melamine-containing food products has severely adverse and even lethal effects on humans (Li, Song, and Wen 2019). Therefore, melamine determination in milk products is so important. For that purpose, numerous MIP chemosensors were devised (Hu and Lu 2016; You, Cao, and Cao 2016; Li, Zheng, et al. 2018; Shang, Zhao, and Zeng 2014; Xu et al. 2018; Shamsipur, Moradi, and Pashabadi 2018; Pietrzyk et al. 2009; Ceylan Cömert et al. 2022).

Another parameter influencing food safety is its freshness. Stale or rotten food not only loses its texture and taste but may harm consumers' health. Therefore, MIP chemosensors for determination of biogenic amines signaling food rottenness, namely histamine (Gao, Grant, and Lu 2015; Mattsson et al. 2018; Wang, Fang, et al. 2017; Jiang et al. 2015; Hassan et al. 2019; Chen, Wang, et al. 2022), and tyramine (Ayerdurai, Cieplak, et al. 2021) were applied for analysis of fish (Gao, Grant, and Lu 2015; Mattsson et al. 2018; Q. H. Wang, Fang, et al. 2017; Jiang et al. 2015; Hassan et al. 2019), prawns (Chen, Wang, et al. 2022), cheese (Ayerdurai, Cieplak, et al. 2021), and vinegar (Chen, Wang, et al. 2022) samples. Moreover, mycotoxins (Bagheri et al. 2018; Munawar et al. 2020; Guo et al. 2017; Pacheco et al. 2015; Gao, Cao, et al. 2014; Qiu et al. 2020; Çimen, Bereli, and Denizli 2022) and bacterial enterotoxins (Liu et al. 2014) indicate the presence of fungi and bacteria, respectively, and bacteria *E. coli* cells by themselves (Cornelis et al. 2019), were determined using MIP chemosensors.

5.1. Miscellaneous applications

Interestingly, MIP chemosensors were applied not only for undesired contaminants determination in food samples but also for food quality assessment. Accordingly, wine astringency was estimated. For that, the LSPR MIP chemosensor imprinted with saliva proteins was designed to study the interactions of these proteins with wine samples (Guerreiro et al. 2017). Presumably, wine ingredients bound saliva proteins, thus causing these proteins to shear and feel dryness. The wine astringency estimated by the MIP chemosensor and expressed in pentagalloyl glucose units (PGG) agreed well with the wine evaluation by a professional taster.

Moreover, flavors (Yang, Zhao, and Zeng 2016; W. H. Wu, Yang, et al. 2017), caffeine (Santos et al. 2012), quercetin (Sun et al. 2013; Yang, Xu, et al. 2017), and necessary nutrients, including vitamins (Feng et al. 2013) or L-phenylalanine (Zhou et al. 2020) were determined with MIP chemosensors to quantify food products quality.

6. Challenges and future prospectives

Polymer synthesis is easily scalable and can be implemented on an industrial scale. Therefore, MIPs can be readily synthesized in the form of bulk polymers, sponges, membranes, micro-, and nanoparticles. Recently, MIP-based SPE columns were introduced to the market. Because of a relatively high price, commercial applications of these MIPs are limited to sample pretreatment in clinical analysis. However, with the increase in the production volume, MIP resins price should

drop so much that they will find applications in the food industry. Possibly, first in veterinary, later in food quality control, and, finally, in food products processing.

However, several important issues should be resolved before implementing the MIPs synthesis in the industry. One deficiency is the necessity of using templates to synthesize MIPs. These templates are removed from MIPs within the final steps of their synthesis and then they are being dumped to waists. Because toxic compounds, i.e., heavy metal ions, mycotoxins, pesticides, antibiotics, and hormones, are usually used as templates, producing waists containing these compounds may constitute a severe risk to human health and the environment. This issue may be resolved by the approach proposed by Piletsky's (Canfarotta et al. 2016)· and Haupt's (Ambrosini et al. 2013; Xu et al. 2016) research groups. Both groups have developed protocols for automated MIP NPs synthesis on solid supports. In this approach, template molecules are immobilized on a glass bead (solid support) surface. Next, MIP NPs are grown around these immobilized templates, and then washed out. Thus, the template stays on the solid support surface and can be used multiple times for MIP NPs synthesis. Moreover, the toxic template does not contaminate synthesized MIP, nor toxic wastes are produced during the synthesis.

The most critical challenge in introducing MIPs to the food processing industry seems to be preventing microplastic contamination. This contamination accompanies any production and application of polymers nowadays. That is, MIPs may be a source of not only microplastic in the environment but also may contaminate processed food products. Microplastic contamination is not only a severe environmental burden but also has significant adverse effects on human health (Rainieri and Barranco 2019; De-la-Torre 2020; Kwon et al. 2020). One solution to this problem is the synthesis of magnetic MIP NPs. Those MIP NPs can be readily removed from samples and collected by simply applying a magnetic field (da Fonseca Alves et al. 2021; Aylaz et al. 2021; Siciliano et al. 2022). Another approach may be to use biodegradable polymers for MIP synthesis. For example, the imprinted chitosan (Zouaoui et al. 2020; Bagheri and Ghaedi 2019), cellulose (Wen et al. 2022; Cao et al. 2021), and crosslinked poly(lactide-*co*-glycolide) dendrimers (Kumar, Jha, and Panda 2019; Gagliardi, Bertero, and Bifone 2017) have already been reported. Moreover, dimeric vanillin derivatives were recently applied as monomers for synthesizing a photodegradable polymer (Singathi et al. 2022). Importantly, this polymer decomposed in a controlled manner into vanillin dimers upon irradiation with UV light of $\lambda = 300$ nm. If it were applied for MIP NPs synthesis, these MIP NPs would be stable until irradiating with the light of the above wavelength. Then, they would decompose to harmless vanillin dimers. Similarly, NPs of polycoumarin were synthesized by irradiation with UV light (Avó, Lima, and Jorge Parola 2019). Importantly, photodimerization of coumarin is a reversible process if it is irradiated with light of a defined wavelength (Wolff and Görner 2010). Therefore, it would also be possible to photodegrade such NPs. However, none of these two polymers has yet been applied in MIP synthesis. Moreover, it is possible to synthesize MIPs from materials that are biocompatible and harmless to the environment. Namely, imprinted polydopamine (Palladino, Bettazzi, and Scarano 2019; Siciliano et al. 2022), polyscopoletin (Bognár et al. 2022; Jetzschmann et al. 2019; Di Giulio, Mazzotta, and Malitesta 2020), and silica (Susanti and Hasanah 2021; Susanti, Mutakin, and Hasanah 2022) were reported. These materials occur in the natural environment and seem to have no adverse influence on living organisms.

Presumably, most of the above challenges are solvable. Notably, the most significant advantage of MIPs fabrication consists in their versatility. That is, if an MIP-based product, e.g., an SPE cartridge, HPLC column, chemosensor, etc., is implemented into mass production, only limited optimization is needed to implement other analogous products selective for other analytes. Therefore, most implementation costs must be covered for the first product in the manufacturer's offer. But if this investment pays off, extending the range of products will be less costly. Therefore, we assume that if MIP-based products mentioned in the present article prove to be a commercial success, within the next few years, the offer of MIP-based analytical tools will be extended, and their price will be significantly reduced. That will open the field for the widespread application of these products.

7. Conclusions

Molecularly imprinted polymers (MIPs) exemplify the idea of smart materials. As selective sorbents, MIPs have recently been introduced to the market. With the increasing number of applications, their cost will decrease, and their availability will increase. Due to their unique properties, including high selectivity and durability, MIPs may find numerous applications in food manufacturing, food safety, and food quality control. MIP-based chemosensors fabrication is a constantly growing field. Several examples of robust, very sensitive, and selective MIP chemosensors reported in the literature suggest that the MIP-using technology is sufficiently mature to enter the market even within the current decade. Hand-held devices, especially those based on visual readout with naked-eye, may find interest from both sides, i.e., end-user customers and farmers who would like to control quality of their food products during production. It is easy to envision that in the not-too-distant future, customers will come to a food market equipped with hand-held analytical devices of the size of a mobile phone, capable of testing the quality of food products on the spot by themselves.

Disclosure statement

We confirm that none of the coauthors has any conflict of interest to be declared.

Funding

The National Science Center of Poland financially supported the present research (Grant SONATA no. 2018/31/D/ST5/02890 to M.C.).

Moreover, the present scientific work was partially funded from the financial resources for science in 2017–2021, awarded by the Polish Ministry of Science and Higher Education for implementing an international co-financed project. Furthermore, the present publication is part of a project that has received funding from the European Union's Horizon 2020 research and innovation program under the Marie Sklodowska-Curie grant agreement No. 711859.

ORCID

Viknasvarri Ayerdurai http://orcid.org/0000-0001-6595-5279
Patrycja Lach http://orcid.org/0000-0002-5009-6560
Agnieszka Lis-Cieplak http://orcid.org/0000-0001-8998-9254
Maciej Cieplak http://orcid.org/0000-0002-2663-7259
Wlodzimierz Kutner http://orcid.org/0000-0003-3586-5170
Piyush Sindhu Sharma http://orcid.org/0000-0002-7729-8314

Abbreviations

AChE	Acetylcholinesterase
ATRP	Atom transfer radical polymerization
bpy	2,2'-Bipyridine
CLB	Clenbuterol
DPV	Differential pulse voltammetry
ECL	Electrochemiluminescence
EG-FET	Extended-gate field-effect transistor
EIS	Electrochemical impedance spectroscopy
ELISA	Enzyme-linked immunosorbent assay
GCE	Glassy carbon electrode
GO	Graphene oxide
GDH	Glucose dehydrogenase
GOx	Glucose oxidase
HPLC	High-performance liquid chromatography
HPLC-MS	High-performance liquid chromatography with mass spectrometry detection
HRP	Horseradish peroxidase
ITO	Indium-tin oxide
LSPR	Localized surface plasmon resonance
MIP	Molecularly imprinted polymer
MOF	Metal-organic framework
MWCNT	Multi-walled carbon nanotube
NP	Nanoparticle
PAH	Polycyclic aromatic hydrocarbon
PDMS	Polydimethylsiloxane
PGG	pentagalloyl glucose unit
PVC	Poly(vinyl chloride)
rGO	Reduced graphene oxide
QCM	Quartz crystal microbalance
QCR	Quartz crystal resonator
QD	Quantum dot
SAM	Self-assembled monolayer
SERS	Surface-enhanced Raman spectroscopy
SPE	Solid-phase extraction
SPR	Surface plasmon resonance
SWCNT	Single-walled carbon nanotube
TLC	Thin-layer chromatography
UCNPs	Upconversion nanoparticles

References

Ali, M. H., and N. Suleiman. 2018. Eleven shades of food integrity: A halal supply chain perspective. *Trends in Food Science & Technology* 71:216–24. doi: 10.1016/j.tifs.2017.11.016.

Altintas, Z. 2018. Surface plasmon resonance based sensor for the detection of glycopeptide antibiotics in milk using rationally designed nanoMIPs. *Scientific Reports* 8:11222. doi. 10.1038/s41598-018-29585-2.

Amatatongchai, M., W. Sroysee, P. Jarujamrus, D. Nacapricha, and P. A. Lieberzeit. 2018. Selective amperometric flow-injection analysis of carbofuran using a molecularly-imprinted polymer and gold-coated-magnetite modified carbon nanotube-paste electrode. *Talanta* 179:700–9. doi: 10.1016/j.talanta.2017.11.064.

Ambrosini, S., S. Beyazit, K. Haupt, and B. T. S. Bui. 2013. Solid-phase synthesis of molecularly imprinted nanoparticles for protein recognition. *Chemical Communications (Cambridge, England)* 49 (60):6746–8.

Anirudhan, T. S., and S. Alexander. 2015. Design and fabrication of molecularly imprinted polymer-based potentiometric sensor from the surface modified multiwalled carbon nanotube for the determination of lindane (gamma-hexachlorocyclohexane), an organochlorine pesticide. *Biosensors & Bioelectronics* 64:586–93. doi: 10.1016/j.bios.2014.09.074.

Antonelli, G., and E. Viganò. 2018. Global challenges in traditional food production and consumption. In *Case studies in the traditional food sector*, by A. Cavicchi and C. Santini, 25–46. Duxford: Woodhead Publishing. doi. 10.1016/B978-0-08-101007-5.00003-8.

Ashley, J., X. T. Feng, and Y. Sun. 2018. A multifunctional molecularly imprinted polymer-based biosensor for direct detection of doxycycline in food samples. *Talanta* 182:49–54. doi: 10.1016/j.talanta.2018.01.056.

Ashley, J., M. A. Shahbazi, K. Kant, V. A. Chidambara, A. Wolff, D. D. Bang, and Y. Sun. 2017. Molecularly imprinted polymers for sample preparation and biosensing in food analysis: Progress and perspectives. *Biosensors & Bioelectronics* 91:606–15. doi: 10.1016/j.bios.2017.01.018.

Ashley, J., Y. Shukor, R. D'Aurelio, L. Trinh, T. L. Rodgers, J. Temblay, M. Pleasants, and I. E. Tothill. 2018. Synthesis of molecularly imprinted polymer nanoparticles for alpha-casein detection using surface plasmon resonance as a milk allergen sensor. *ACS Sensors* 3 (2):418–24. doi: 10.1021/acssensors.7b00850.

Athikomrattanakul, U., N. Gajovic-Eichelmann, and F. W. Scheller. 2011. Thermometric sensing of nitrofurantoin by noncovalently imprinted polymers containing two complementary functional monomers. *Analytical Chemistry* 83 (20):7704–11. doi: 10.1021/ac201099h.

Avó, J., J. C. Lima, and A. Jorge Parola. 2019. Photo-controlled growth of polymeric submicron-sized particles. *Photochemical & Photobiological Sciences* 18 (5):993–6. doi: 10.1039/c9pp00086k.

Ayerdurai, V., M. Cieplak, K. R. Noworyta, M. Gajda, A. Ziminska, M. Sosnowska, J. Piechowska, P. Borowicz, W. Lisowski, S. Shao, et al. 2021. Electrochemical sensor for selective tyramine determination, amplified by a molecularly imprinted polymer film. *Bioelectrochemistry* 138:107695. doi: 10.1016/j.bioelechem.2020.107695.

Ayerdurai, V., A. Garcia-Cruz, J. Piechowska, M. Cieplak, P. Borowicz, K. R. Noworyta, G. Spolnik, W. Danikiewicz, W. Lisowski, A. Pietrzyk-Le, et al. 2021. Selective impedimetric chemosensing of carcinogenic heterocyclic aromatic amine in pork by dsDNA-mimicking molecularly imprinted polymer film-coated electrodes. *Journal of Agricultural and Food Chemistry* 69 (48):14689–98. doi: 10.1021/acs.jafc.1c05084.

Aylaz, G., J. Kuhn, E. C. H. T. Lau, C. Yeung, V. A. L. Roy, M. Duman, and H. H. P. Yiu. 2021. Recent developments on magnetic molecular imprinted polymers (MMIPs) for sensing, capturing, and monitoring pharmaceutical and agricultural pollutants. *Journal of Chemical Technology & Biotechnology* 96 (5):1151–60. doi: 10.1002/jctb.6681.

Bagheri, A. R., and M. Ghaedi. 2019. Synthesis of chitosan based molecularly imprinted polymer for pipette-tip solid phase extraction of Rhodamine B from chili powder samples. *International Journal of Biological Macromolecules* 139:40–8. doi: 10.1016/j.ijbiomac.2019.07.196.

Bagheri, N., A. Khataee, B. Habibi, and J. Hassanzadeh. 2018. Mimetic Ag nanoparticle/Zn-based MOF nanocomposite (AgNPs@ZnMOF) capped with molecularly imprinted polymer for the selective detection of patulin. *Talanta* 179:710–8. doi: 10.1016/j.talanta.2017.12.009.

Bai, J. L., X. Y. Zhang, Y. Peng, X. D. Hong, Y. Y. Liu, S. Y. Jiang, B. A. Ning, and Z. X. Gao. 2017. Ultrasensitive sensing of diethylstilbestrol based on AuNPs/MWCNTs-CS composites coupling with sol-gel molecularly imprinted polymer as a recognition element of an electrochemical sensor. *Sensors and Actuators B: Chemical* 238:420–6. doi: 10.1016/j.snb.2016.07.035.

Beyazit, S., B. T. S. Bui, K. Haupt, and C. Gonzato. 2016. Molecularly imprinted polymer nanomaterials and nanocomposites by controlled/living radical polymerization. *Progress in Polymer Science* 62:1–21. doi: 10.1016/j.progpolymsci.2016.04.001.

Blasco, C., and Y. Pico. 2012. Development of an improved method for trace analysis of quinolones in eggs of laying hens and wildlife species using molecularly imprinted polymers. *Journal of Agricultural and Food Chemistry* 60 (44):11005–14. doi: 10.1021/jf303222a.

Bognár, Z., E. Supala, A. Yarman, X. Zhang, F. F. Bier, F. W. Scheller, and R. E. Gyurcsányi. 2022. Peptide epitope-imprinted polymer microarrays for selective protein recognition. Application for SARS-CoV-2 RBD protein. *Chemical Science* 13 (5):1263–9. doi: 10.1039/d1sc04502d.

Bousoumah, R., J. P. Antignac, V. Camel, M. Grimaldi, P. Balaguer, F. Courant, E. Bichon, M. L. Morvan, and B. L. Bizec. 2015. Development of a molecular recognition based approach for multi-residue extraction of estrogenic endocrine disruptors from biological fluids coupled to liquid chromatography-tandem mass spectrometry measurement. *Analytical and Bioanalytical Chemistry* 407 (29):8713–23. doi: 10.1007/s00216-015-9024-4.

Bryła, M., R. Jędrzejczak, M. Roszko, K. Szymczyk, M. W. Obiedziński, J. Sękul, and M. Rzepkowska. 2013. Application of molecularly imprinted polymers to determine B-1, B-2, and B-3 fumonisins in cereal products. *Journal of Separation Science* 36 (3):578–84. doi: 10.1002/jssc.201200753.

Bustamante-Rangel, M., E. Rodríguez-Gonzalo, and M. M. Delgado-Zamareño. 2022. Evaluation of the selectivity of molecularly imprinted polymer cartridges for nitroimidazoles. Application to the simultaneous extraction of nitroimidazoles and benzimidazoles from samples of animal origin. *Microchemical Journal* 172:107000. doi: 10.1016/j.microc.2021.107000.

Canfarotta, F., A. Poma, A. Guerreiro, and S. Piletsky. 2016. Solid-phase synthesis of molecularly imprinted nanoparticles. *Nature Protocols* 11 (3):443–55. doi: 10.1038/nprot.2016.030.

Cao, J. L., W. J. Kong, S. J. Zhou, L. H. Yin, L. Wan, and M. H. Yang. 2013. Molecularly imprinted polymer-based solid phase clean-up for analysis of ochratoxin A in beer, red wine, and grape juice. *Journal of Separation Science* 36 (7):1291–7. doi: 10.1002/jssc.201201055.

Cao, J. L., S. J. Zhou, W. J. Kong, M. H. Yang, L. Wan, and S. H. Yang. 2013. Molecularly imprinted polymer-based solid phase clean-up for analysis of ochratoxin A in ginger and LC-MS/MS confirmation. *Food Control* 33 (2):337–43. doi: 10.1016/j.foodcont.2013.03.023.

Cao, J., C. Shen, X. Wang, Y. Zhu, S. Bao, X. Wu, and Y. Fu. 2021. A porous cellulose-based molecular imprinted polymer for specific recognition and enrichment of resveratrol. *Carbohydrate Polymers* 251:117026. doi: 10.1016/j.carbpol.2020.117026.

Capoferri, D., M. Del Carlo, N. Ntshongontshi, E. I. Iwuoha, M. Sergi, F. D. Ottavio, and D. Compagnone. 2017. MIP-MEPS based sensing strategy for the selective assay of dimethoate. Application to wheat flour samples. *Talanta* 174:599–604. doi: 10.1016/j.talanta.2017.06.062.

Catana, M., L. Catana, E. Iorga, A. C. Asanica, A. G. Lazar, M. A. Lazar, N. Belc, and G. Pirvu. 2019. Internal validation of rapid and performance method for patulin determination in apple cider by high-performance liquid chromatography. *Revista de Chimie* 70 (11):3921–5. doi: 10.37358/RC.19.11.7673.

Ceylan Cömert, Ş., E. Özgür, L. Uzun, and M. Odabaşı. 2022. The creation of selective imprinted cavities on quartz crystal microbalance electrode for the detection of melamine in milk sample. *Food Chemistry* 372:131254. doi: 10.1016/j.foodchem.2021.131254.

Chen, C., and J. S. Wang. 2020. Optical biosensors: An exhaustive and comprehensive review. *The Analyst* 145 (5):1605–28. doi: 10.1039/c9an01998g.

Chen, C., X. Wang, G. I. N. Waterhouse, X. Qiao, and Z. Xu. 2022. A surface-imprinted surface-enhanced Raman scattering sensor for histamine detection based on dual semiconductors and Ag nanoparticles. *Food Chemistry* 369:130971. doi: 10.1016/j.foodchem.2021.130971.

Chen, S., J. Fu, S. Zhou, P. Zhao, X. Wu, S. Tang, and Z. Zhang. 2022. Rapid recognition of di-n-butyl phthalate in food samples with a near infrared fluorescence imprinted sensor based on zeolite imidazolate framework-67. *Food Chemistry* 367:130505. doi: 10.1016/j.foodchem.2021.130505.

Cieplak, M., and W. Kutner. 2016. Artificial biosensors: How can molecular imprinting mimic biorecognition? *Trends in Biotechnology* 34 (11):922–41. doi: 10.1016/j.tibtech.2016.05.011.

Çimen, D., N. Bereli, and A. Denizli. 2022. Patulin imprinted nanoparticles decorated surface plasmon resonance chips for patulin detection. *Photonic Sensors* 12 (2):117–29. doi: 10.1007/s13320-021-0638-1.

Cirkva, A., I. Malkova, M. Rejtharova, E. Vernerova, A. Hera, and J. Bures. 2019. Residue study of nitroimidazoles depletion in chicken feathers in comparison with some other selected matrixes. *Food Additives & Contaminants, Part A, Chemistry, Analysis, Control, Exposure & Risk Assessment* 36 (8):1206–17. doi: 10.1080/19440049.2019.1627000.

Cornelis, P., S. Givanoudi, D. Yongabi, H. Iken, S. Duwé, O. Deschaume, J. Robbens, P. Dedecker, C. Bartic, M. Wübbenhorst, et al. 2019. Sensitive and specific detection of E. coli using biomimetic receptors in combination with a modified heat-transfer method. *Biosensors & Bioelectronics* 136:97–105. doi: 10.1016/j.bios.2019.04.026.

Cui, Z. M., Z. Y. Li, Y. T. Jin, T. T. Ren, J. A. Chen, X. H. Wang, K. L. Zhong, L. J. Tang, Y. W. Tang, and M. R. Cao. 2020. Novel magnetic fluorescence probe based on carbon quantum dots-doped molecularly imprinted polymer for AHLs signaling molecules sensing in fish juice and milk. *Food Chemistry* 328:127063. doi: 10.1016/j.foodchem.2020.127063.

da Fonseca Alves, R., L. Neres Chagas da Silva, G. M. Neto, I. F. Ierick, T. L. Ferreira and M. D. P. T. Sotomayor. 2021. Magnetic MIPs: Synthesis and applications. In *Molecularly imprinted polymers, Methods in Molecular Biology,* by A. Martín-Esteban, 85–96. New York: Humana.

Dabrowski, M., P. S. Sharma, Z. Iskierko, K. Noworyta, M. Cieplak, W. Lisowski, S. Oborska, A. Kuhn, and W. Kutner. 2016. Early diagnosis of fungal infections using piezomicrogravimetric and electric chemosensors based on polymers molecularly imprinted with D-arabitol. *Biosensors & Bioelectronics* 79:627–35. doi: 10.1016/j.bios.2015.12.088.

Dadkhah, S., E. Ziaei, A. Mehdinia, T. B. Kayyal, and A. Jabbari. 2016. A glassy carbon electrode modified with amino-functionalized graphene oxide and molecularly imprinted polymer for electrochemical sensing of bisphenol A. *Microchimica Acta* 183 (6):1933–41. doi: 10.1007/s00604-016-1824-5.

Dayal, H., W. Y. Ng, X. H. Lin, and S. F. Y. Li. 2019. Development of a hydrophilic molecularly imprinted polymer for the detection of hydrophilic targets using quartz crystal microbalance. *Sensors and Actuators B: Chemical* 300:127044. doi: 10.1016/j.snb.2019.127044.

De-la-Torre, G. E. 2020. Microplastics: An emerging threat to food security and human health. *Journal of Food Science and Technology* 57 (5):1601–8. doi: 10.1007/s13197-019-04138-1.

Deceuninck, Y., E. Bichon, P. Marchand, C. Y. Boquien, A. Legrand, C. Boscher, J. P. Antignac, and B. L. Bizec. 2015. Determination of bisphenol A and related substitutes/analogues in human breast milk using gas chromatography-tandem mass spectrometry. *Analytical and Bioanalytical Chemistry* 407 (9):2485–97. doi: 10.1007/s00216-015-8469-9.

Deng, P. H., Z. F. Xu, and Y. F. Kuang. 2014. Electrochemical determination of bisphenol A in plastic bottled drinking water and canned beverages using a molecularly imprinted chitosan-graphene composite film modified electrode. *Food Chemistry* 157:490–7. doi: 10.1016/j.foodchem.2014.02.074.

Di Giulio, T., E. Mazzotta, and C. Malitesta. 2020. Molecularly imprinted polyscopoletin for the electrochemical detection of the chronic disease marker lysozyme. *Biosensors* 11 (1):3. doi: 10.3390/bios11010003.

Ebarvia, B. S., I. E. Ubando, and F. B. Sevilla. 2015. Biomimetic piezoelectric quartz crystal sensor with chloramphenicol-imprinted polymer sensing layer. *Talanta* 144:1260–5. doi: 10.1016/j.talanta.2015.08.001.

Fang, G. Z., Y. K. Yang, H. D. Zhu, Y. Qi, J. M. Liu, H. L. Liu, and S. Wang. 2017. Development and application of molecularly imprinted quartz crystal microbalance sensor for rapid detection of metolcarb in foods. *Sensors and Actuators B: Chemical* 251:720–8. doi: 10.1016/j.snb.2017.05.094.

Fang, M., L. Zhou, H. Zhang, L. Liu, and Z. Y. Gong. 2019. A molecularly imprinted polymers/carbon dots-grafted paper sensor for 3-monochloropropane-1,2-diol determination. *Food Chemistry* 274:156–61. doi: 10.1016/j.foodchem.2018.08.133.

Feng, J. Y., Y. X. Hu, E. Grant, and X. N. Lu. 2018. Determination of thiabendazole in orange juice using an MISPE-SERS chemosensor. *Food Chemistry* 239:816–22. doi: 10.1016/j.foodchem.2017.07.014.

Feng, S. L., F. Gao, Z. W. Chen, E. Grant, D. D. Kitts, S. Wang, and X. N. Lu. 2013. Determination of alpha-tocopherol in vegetable oils using a molecularly imprinted polymers-surface-enhanced Raman spectroscopic biosensor. *Journal of Agricultural and Food Chemistry* 61 (44):10467–75. doi: 10.1021/jf4038858.

Feng, S. L., Y. X. Hu, L. Y. Ma, and X. N. Lu. 2017. Development of molecularly imprinted polymers-surface-enhanced Raman spectroscopy/colorimetric dual sensor for determination of chlorpyrifos in apple juice. *Sensors and Actuators B: Chemical* 241:750–7. doi: 10.1016/j.snb.2016.10.131.

Futra, D., L. Y. Heng, M. Z. Jaapar, A. Ulianas, K. Saeedfar, and T. L. Ling. 2016. A novel electrochemical sensor for 17 beta-estradiol from molecularly imprinted polymeric microspheres and multi-walled carbon nanotubes grafted with gold nanoparticles. *Analytical Methods* 8 (6):1381–9. doi: 10.1039/C5AY02796A.

Gagliardi, M., A. Bertero, and A. Bifone. 2017. Molecularly imprinted biodegradable nanoparticles. *Scientific Reports* 7:40046. doi: 10.1038/srep40046.

Gao, F., E. Grant, and X. N. Lu. 2015. Determination of histamine in canned tuna by molecularly imprinted polymers-surface enhanced Raman spectroscopy. *Analytica Chimica Acta* 901:68–75. doi: 10.1016/j.aca.2015.10.025.

Gao, F., Y. X. Hu, D. Chen, E. C. Y. Li-Chan, E. Grant, and X. N. Lu. 2015. Determination of Sudan I in paprika powder by molecularly imprinted polymers-thin layer chromatography-surface enhanced Raman spectroscopic biosensor. *Talanta* 143:344–52. doi: 10.1016/j.talanta.2015.05.003.

Gao, L., X. Y. Li, Q. Zhang, J. D. Dai, X. Wei, Z. L. Song, Y. S. Yan, and C. X. Li. 2014. Molecularly imprinted polymer microspheres for optical measurement of ultra trace nonfluorescent cyhalothrin in honey. *Food Chemistry* 156:1–6. doi: 10.1016/j.foodchem.2013.12.065.

Gao, X., W. Y. Cao, M. M. Chen, H. Y. Xiong, X. H. Zhang, and S. F. Wang. 2014. A high sensitivity electrochemical sensor based on Fe^{3+}-ion molecularly imprinted film for the detection of T-2 toxin. *Electroanalysis* 26 (12):2739–46. doi: 10.1002/elan.201400237.

Gonzalez-Salamo, J., B. Socas-Rodriguez, J. Hernandez-Borges, M. D. Afonso, and M. A. Rodriguez-Delgado. 2015. Evaluation of two molecularly imprinted polymers for the solid-phase extraction of natural, synthetic and mycoestrogens from environmental water samples before liquid chromatography with mass spectrometry. *Journal of Separation Science* 38:2692–9.

Guerreiro, J. R. L., N. Teixeira, V. De Freitas, M. G. F. Sales, and D. S. Sutherland. 2017. A saliva molecular imprinted localized surface plasmon resonance biosensor for wine astringency estimation. *Food Chemistry* 233:457–66. doi: 10.1016/j.foodchem.2017.04.051.

Guo, W., F. W. Pi, H. X. Zhang, J. D. Sun, Y. Z. Zhang, and X. L. Sun. 2017. A novel molecularly imprinted electrochemical sensor modified with carbon dots, chitosan, gold nanoparticles for the determination of patulin. *Biosensors & Bioelectronics* 98:299–304. doi: 10.1016/j.bios.2017.06.036.

Hassan, A. H. A., L. Sappia, S. L. Moura, F. H. M. Ali, W. A. Moselhy, M. D. T. Sotomayor, and M. I. Pividori. 2019. Biomimetic magnetic sensor for electrochemical determination of scombrotoxin in fish. *Talanta* 194:997–1004. doi: 10.1016/j.talanta.2018.10.066.

Hrobonova, K., and E. Brokesova. 2020. Comparison of different types of sorbents for extraction of coumarins. *Food Chemistry* 332:127404.

Hu, Y. X., and X. N. Lu. 2016. Rapid detection of melamine in tap water and milk using conjugated "One-Step" molecularly imprinted polymers-surface enhanced Raman spectroscopic sensor. *Journal of Food Science* 81 (5):N1272–N1280. doi: 10.1111/1750-3841.13283.

Hua, M. Z., S. L. Feng, S. Wang, and X. N. Lu. 2018. Rapid detection and quantification of 2,4-dichlorophenoxyacetic acid in milk using molecularly imprinted polymers-surface-enhanced Raman spectroscopy. *Food Chemistry* 258:254–9. doi: 10.1016/j.foodchem.2018.03.075.

Iskierko, Z., P. S. Sharma, K. R. Noworyta, P. Borowicz, M. Cieplak, W. Kutner, and A. M. Bossi. 2019. Selective PQQPFPQQ gluten epitope chemical sensor with a molecularly imprinted polymer recognition unit and an extended-gate field-effect transistor transduction unit. *Analytical Chemistry* 91 (7):4537–43. doi: 10.1021/acs.analchem.8b05557.

Iskierko, Z., P. S. Sharma, D. Prochowicz, K. Fronc, F. D'Souza, D. Toczydłowska, F. Stefaniak, and K. Noworyta. 2016. Molecularly imprinted polymer (MIP) film with improved surface area developed by using metal-organic framework (MOF) for sensitive lipocalin (NGAL) determination. *ACS Applied Materials & Interfaces* 8 (31):19860–5. doi: 10.1021/acsami.6b05515.

Jalili, R., A. Khataee, M. R. Rashidi, and A. Razmjou. 2020. Detection of penicillin G residues in milk based on dual-emission carbon dots and molecularly imprinted polymers. *Food Chemistry* 314:126172. doi: 10.1016/j.foodchem.2020.126172.

Jetzschmann, K. J., S. Tank, G. Jágerszki, R. E. Gyurcsányi, U. Wollenberger, and F. W. Scheller. 2019. Bio-electrosynthesis of vectorially imprinted polymer nanofilms for Cytochrome P450cam. *ChemElectroChem* 6 (6):1818–23. doi: 10.1002/celc.201801851.

Jiang, S. Y., Y. Peng, B. A. Ning, J. L. Bai, Y. Y. Liu, N. Zhang, and Z. X. Gao. 2015. Surface plasmon resonance sensor based on molecularly imprinted polymer film for detection of histamine. *Sensors and Actuators B: Chemical* 221:15–21. doi: 10.1016/j.snb.2015.06.058.

Jin, X. C., G. Z. Fang, M. F. Pan, Y. K. Yang, X. Y. Bai, and S. Wang. 2018. A molecularly imprinted electrochemiluminescence sensor based on upconversion nanoparticles enhanced by electrodeposited rGO for selective and ultrasensitive detection of clenbuterol. *Biosensors & Bioelectronics* 102:357–64. doi: 10.1016/j.bios.2017.11.016.

Khanmohammadi, A., A. Aghaie, E. Vahedi, A. Qazvini, M. Ghanei, A. Afkhami, A. Hajian, and H. Bagheri. 2020. Electrochemical biosensors for the detection of lung cancer biomarkers: A review. *Talanta* 206:120251. doi: 10.1016/j.talanta.2019.120251.

Kubiak, A., A. Ciric, and M. Biesaga. 2020. Dummy molecularly imprinted polymer (DMIP) as a sorbent for bisphenol S and bisphenol F extraction from food samples. *Microchemical Journal* 156:104836. doi: 10.1016/j.microc.2020.104836.

Kumar, R., D. Jha, and A. K. Panda. 2019. Antimicrobial therapeutics delivery systems based on biodegradable polylactide/polylactide-co-glycolide particles. *Environmental Chemistry Letters* 17 (3):1237–49. doi: 10.1007/s10311-019-00871-3.

Kupai, J., M. Razali, S. Buyuktiryaki, R. Kecili, and G. Szekely. 2017. Long-term stability and reusability of molecularly imprinted polymers. *Polymer Chemistry* 8 (4):666–73. doi: 10.1039/c6py01853j.

Kwon, J.-H., J.-W. Kim, T. D. Pham, A. Tarafdar, S. Hong, S.-H. Chun, S.-H. Lee, D.-Y. Kang, J.-Y. Kim, S.-B. Kim, et al. 2020. Microplastics in food: A review on analytical methods and challenges. *International Journal of Environmental Research and Public Health* 17 (18):6710. doi: 10.3390/ijerph17186710.

Lach, P., M. Cieplak, M. Majewska, K. R. Noworyta, P. S. Sharma, and W. Kutner. 2019. "Gate effect" in *p*-synephrine electrochemical sensing with a molecularly imprinted polymer and redox probes. *Analytical Chemistry* 91 (12):7546–53. doi: 10.1021/acs.analchem.8b05512.

Lach, P., M. Cieplak, K. R. Noworyta, P. Pieta, W. Lisowski, J. Kalecki, R. Chitta, F. D'Souza, W. Kutner, and P. S. Sharma. 2021. Self-reporting molecularly imprinted polymer with the covalently immobilized ferrocene redox probe for selective electrochemical sensing of *p*-synephrine. *Sensors and Actuators B: Chemical* 344:130276. doi: 10.1016/j.snb.2021.130276.

Lach, P., P. S. Sharma, K. Golebiewska, M. Cieplak, F. D'Souza, and W. Kutner. 2017. Molecularly imprinted polymer chemosensor for selective determination of an *N*-nitroso-L-proline food toxin. *Chemistry (Weinheim an Der Bergstrasse, Germany)* 23 (8):1942–9. doi: 10.1002/chem.201604799.

Li, H., and L. Y. Wang. 2013. Highly selective detection of polycyclic aromatic hydrocarbons using multifunctional magnetic-luminescent molecularly imprinted polymers. *ACS Applied Materials & Interfaces* 5 (21):10502–9. doi: 10.1021/am4020605.

Li, J. B., X. J. Wang, H. M. Duan, Y. H. Wang, Y. N. Bu, and C. N. Luo. 2016. Based on magnetic graphene oxide highly sensitive and selective imprinted sensor for determination of sunset yellow. *Talanta* 147:169–76. doi: 10.1016/j.talanta.2015.09.056.

Li, J. H., Z. F. Xu, M. Q. Liu, P. H. Deng, S. P. Tang, J. B. Jiang, H. B. Feng, D. Qian, and L. Z. He. 2017. Ag/N-doped reduced graphene oxide incorporated with molecularly imprinted polymer: An advanced electrochemical sensing platform for salbutamol determination. *Biosensors & Bioelectronics* 90:210–6. doi: 10.1016/j.bios.2016.11.016.

Li, L., Z. Z. Lin, Z. Y. Huang, and A. H. Peng. 2019. Rapid detection of sulfaguanidine in fish by using a photonic crystal molecularly imprinted polymer. *Food Chemistry* 281:57–62. doi: 10.1016/j.foodchem.2018.12.073.

Li, Q., P. Song, and J. Wen. 2019. Melamine and food safety: A 10-year review. *Current Opinion in Food Science* 30:79–84. doi: 10.1016/j.cofs.2019.05.008.

Li, S. H., J. P. Li, J. H. Luo, Z. Xu, and X. H. Ma. 2018. A microfluidic chip containing a molecularly imprinted polymer and a DNA aptamer for voltammetric determination of carbofuran. *Microchimica Acta* 185 (6):295.

Li, S. H., C. H. Liu, G. H. Yin, J. H. Luo, Z. S. Zhang, and Y. X. Xie. 2016. Supramolecular imprinted electrochemical sensor for the neonicotinoid insecticide imidacloprid based on double amplification by Pt-In catalytic nanoparticles and a Bromophenol blue doped molecularly imprinted film. *Microchimica Acta* 183 (12):3101–9. doi: 10.1007/s00604-016-1962-9.

Li, S. H., C. H. Liu, G. H. Yin, Q. Zhang, J. H. Luo, and N. C. Wu. 2017. Aptamer-molecularly imprinted sensor base on electrogenerated chemiluminescence energy transfer for detection of lincomycin. *Biosensors & Bioelectronics* 91:687–91. doi: 10.1016/j.bios.2017.01.038.

Li, S. H., G. H. Yin, Q. Zhang, C. L. Li, J. H. Luo, Z. Xu, and A. L. Qin. 2015. Selective detection of fenaminosulf via a molecularly imprinted fluorescence switch and silver nano-film amplification. *Biosensors & Bioelectronics* 71:342–7. doi: 10.1016/j.bios.2015.04.066.

Li, W., Y. P. Zheng, T. W. Zhang, S. J. Wu, J. Zhang, and J. Fang. 2018. A surface plasmon resonance-based optical fiber probe fabricated with electropolymerized molecular imprinting film for melamine detection. *Sensors* 18 (3):828. doi: 10.3390/s18030828.

Li, X. J., H. F. Jiao, X. Z. Shi, A. L. Sun, X. J. Wang, J. Y. Chai, D. X. Li, and J. Chen. 2018. Development and application of a novel fluorescent nanosensor based on FeSe quantum dots embedded silica molecularly imprinted polymer for the rapid optosensing of cyfluthrin. *Biosensors and Bioelectronics* 99:268–73. doi: 10.1016/j.bios.2017.07.071.

Li, Y. C., Y. Liu, Y. Yang, F. Yu, J. Liu, H. Song, J. Liu, H. Tang, B. C. Ye, and Z. P. Sun. 2015. Novel electrochemical sensing platform based on a molecularly imprinted polymer decorated 3D nanoporous nickel skeleton for ultrasensitive and selective determination of metronidazole. *ACS Applied Materials & Interfaces* 7 (28):15474–80. doi: 10.1021/acsami.5b03755.

Lian, W. J., S. Liu, J. H. Yu, J. Li, M. Cui, W. Xu, and J. D. Huang. 2013. Electrochemical sensor using neomycin-imprinted film as recognition element based on chitosan-silver nanoparticles/graphene-multiwalled carbon nanotubes composites modified electrode. *Biosensors & Bioelectronics* 44:70–6. doi: 10.1016/j.bios.2013.01.002.

Lin, X. H., S. X. L. Aik, J. Angkasa, Q. H. Le, K. S. Chooi, and S. F. Y. Li. 2018. Selective and sensitive sensors based on molecularly imprinted poly(vinylidene fluoride) for determination of pesticides and chemical threat agent simulants. *Sensors and Actuators B: Chemical* 258:228–37. doi: 10.1016/j.snb.2017.11.070.

Liu, J., Y. Xu, S. Liu, S. Yu, Z. Yu, and S. S. Low. 2022. Application and progress of chemometrics in voltammetric biosensing. *Biosensors* 12 (7):494. doi: 10.3390/bios12070494.

Liu, N., X. L. Li, X. H. Ma, G. R. Ou, and Z. X. Gao. 2014. Rapid and multiple detections of staphylococcal enterotoxins by two-dimensional molecularly imprinted film-coated QCM sensor. *Sensors and Actuators B: Chemical* 191:326–31. doi: 10.1016/j.snb.2013.09.086.

Liu, X. Y., J. Ren, L. H. Su, X. Gao, Y. W. Tang, T. Ma, L. J. Zhu, and J. R. Li. 2017. Novel hybrid probe based on double recognition of aptamer-molecularly imprinted polymer grafted on upconversion nanoparticles for enrofloxacin sensing. *Biosensors & Bioelectronics* 87:203–8. doi: 10.1016/j.bios.2016.08.051.

Liu, Z. Y., Y. Zhang, J. H. Feng, Q. Z. Han, and Q. Wei. 2019. Ni(OH)(2) nanoarrays based molecularly imprinted polymer electrochemical sensor for sensitive detection of sulfapyridine. *Sensors and Actuators B: Chemical* 287:551–6. doi: 10.1016/j.snb.2019.02.079.

Lu, C., Z. Tang, C. Liu, and X. Ma. 2018. Surface molecularly imprinted polymers prepared by two-step precipitation polymerization for the selective extraction of oleanolic acid from grape pomace extract. *Journal of Separation Science* 41 (17):3496–502. doi: 10.1002/jssc.201800474.

Lucci, P., D. Derrien, F. Alix, C. Perollier, and S. Bayoudh. 2010. Molecularly imprinted polymer solid-phase extraction for detection of zearalenone in cereal sample extracts. *Analytica Chimica Acta* 672 (1–2):15–9. doi: 10.1016/j.aca.2010.03.010.

Matejicek, D., A. Grycova, and J. Vlcek. 2013. The use of molecularly imprinted polymers for the multicomponent determination of endocrine-disrupting compounds in water and sediment. *Journal of Separation Science* 36:1097–103.

Mattsson, L., J. J. Xu, C. Preininger, B. T. S. Bui, and K. Haupt. 2018. Competitive fluorescent pseudo-immunoassay exploiting molecularly imprinted polymers for the detection of biogenic amines in fish matrix. *Talanta* 181:190–6. doi: 10.1016/j.talanta.2018.01.010.

Mier, A., S. Nestora, P. X. M. Rangel, Y. Rossez, K. Haupt, and B. T. S. Bui. 2019. Cytocompatibility of molecularly imprinted polymers for deodorants: Evaluation on human keratinocytes and axillary-hosted bacteria. *ACS Applied Bio Materials* 2 (8):3439–47. doi: 10.1021/acsabm.9b00388.

Munawar, H., A. Garcia-Cruz, M. Majewska, K. Karim, W. Kutner, and S. A. Piletsky. 2020. Electrochemical determination of fumonisin B1 using a chemosensor with a recognition unit comprising molecularly imprinted polymer nanoparticles. *Sensors and Actuators B: Chemical* 321:128552. doi: 10.1016/j.snb.2020.128552.

Naresh, V., and N. Lee. 2021. A review on biosensors and recent development of nanostructured materials-enabled biosensors. *Sensors* 21 (4):1109. doi: 10.3390/s21041109.

Nelis, J. L. D., A. S. Tsagkaris, M. J. Dillon, J. Hajslova, and C. T. Elliott. 2020. Smartphone-based optical assays in the food safety field. *Trends in Analytical Chemistry: TRAC* 129:115934. doi: 10.1016/j.trac.2020.115934.

Nestora, S., F. Merlier, S. Beyazit, E. Prost, L. Duma, B. Baril, A. Greaves, K. Haupt, and B. T. S. Bui. 2016. Plastic antibodies for cosmetics: Molecularly imprinted polymers scavenge precursors of malodors. *Angewandte Chemie (International ed. in English)* 55 (21):6252–6. doi: 10.1002/anie.201602076.

Nicolucci, C., S. Rossi, C. Menale, E. M. del Giudice, L. Perrone, P. Gallo, D. G. Mita, and N. Diano. 2013. A high selective and sensitive liquid chromatography-tandem mass spectrometry method for quantization of BPA urinary levels in children. *Analytical and Bioanalytical Chemistry* 405 (28):9139–48.

Niu, M. C., P. H. Chuong, and H. He. 2016. Core-shell nanoparticles coated with molecularly imprinted polymers: A review. *Microchimica Acta* 183 (10):2677–95. doi: 10.1007/s00604-016-1930-4.

Pacheco, J. G., M. Castro, S. Machado, M. F. Barroso, H. P. A. Nouws, and C. Delerue-Matos. 2015. Molecularly imprinted electrochemical sensor for ochratoxin A detection in food samples. *Sensors and Actuators B: Chemical* 215:107–12. doi: 10.1016/j.snb.2015.03.046.

Pakade, V., E. Cukrowska, S. Lindahl, C. Turner, and L. Chimuka. 2013. Molecular imprinted polymer for solid-phase extraction of flavonol aglycones from Moringa oleifera extracts. *Journal of Separation Science* 36 (3):548–55. doi: 10.1002/jssc.201200576.

Palladino, P., F. Bettazzi, and S. Scarano. 2019. Polydopamine: Surface coating, molecular imprinting, and electrochemistry—successful applications and future perspectives in (bio)analysis. *Analytical and Bioanalytical Chemistry* 411 (19):4327–38. doi: 10.1007/s00216-019-01665-w.

Petcu, M. 2013. Polymer and method of use. WO 2013190506, Jun 21.

Petcu, M. 2015. Polymer and method of use. US 20150361203, Dec 17.

Pieta, P., I. Obraztsov, J. W. Sobczak, O. Chernyayeva, S. K. Das, F. D'Souza, and W. Kutner. 2013. A versatile material for a symmetrical electric energy storage device: A composite of the polymer of the ferrocene adduct of C-60 and single-wall carbon nanotubes exhibiting redox conductivity at both positive and negative potentials. *The Journal of Physical Chemistry C* 117 (5):1995–2007. doi: 10.1021/jp210450y.

Pietrzyk, A., W. Kutner, R. Chitta, M. E. Zandler, F. D'Souza, F. Sannicolo, and P. R. Mussini. 2009. Melamine acoustic chemosensor based on molecularly imprinted polymer film. *Analytical Chemistry* 81 (24):10061–70. doi: 10.1021/ac9020352.

Qi, P., J. Wang, Z. Wang, X. Wang, X. Wang, X. Xu, H. Xu, S. Di, H. Zhang, Q. Wang, et al. 2018. Construction of a probe-immobilized molecularly imprinted electrochemical sensor with dual signal amplification of thiol graphene and gold nanoparticles for selective detection of tebuconazole in vegetable and fruit samples. *Electrochimica Acta* 274:406–14. doi: 10.1016/j.electacta.2018.04.128.

Qin, R. Z., Q. L. Wang, C. Q. Ren, X. Z. Dai, and H. J. Han. 2017. Development of a molecularly imprinted electrochemical sensor for *tert*-butylhydroquinone recognition. *International Journal of Electrochemical Science* 12:8953–62. doi: 10.20964/2017.10.04.

Qiu, X. Z., W. M. Chen, Y. L. Luo, Y. L. Wang, Y. L. Wang, and H. S. Guo. 2020. Highly sensitive alpha-amanitin sensor based on molecularly imprinted photonic crystals. *Analytica Chimica Acta* 1093:142–9. doi: 10.1016/j.aca.2019.09.066.

Rainieri, S., and A. Barranco. 2019. Microplastics, a food safety issue? *Trends in Food Science and Technology* 84:55–7. doi: 10.1016/j.tifs.2018.12.009.

Roszko, M., K. Szymczyk, and R. Jędrzejczak. 2015. Simultaneous separation of chlorinated/brominated dioxins, polychlorinated biphenyls, polybrominated diphenyl ethers and their methoxylated derivatives from hydroxylated analogues on molecularly imprinted polymers prior to gas/liquid chromatography and mass spectrometry. *Talanta* 144:171–83. doi: 10.1016/j.talanta.2015.04.070.

Sa-nguanprang, S., A. Phuruangrat, and O. Bunkoed. 2022. An optosensor based on a hybrid sensing probe of mesoporous carbon and quantum dots embedded in imprinted polymer for ultrasensitive detection of thiamphenicol in milk. *Spectrochimica Acta Part A: Molecular and Biomolecular Spectroscopy* 264:120324. doi: 10.1016/j.saa.2021.120324.

Santos, W. D. R., M. Santhiago, I. V. P. Yoshida, and L. T. Kubota. 2012. Electrochemical sensor based on imprinted sol-gel and nanomaterial for determination of caffeine. *Sensors and Actuators B: Chemical* 166–167:739–45. doi: 10.1016/j.snb.2012.03.051.

Shamsipur, M., N. Moradi, and A. Pashabadi. 2018. Coupled electrochemical-chemical procedure used in construction of molecularly imprinted polymer-based electrode: A highly sensitive impedimetric melamine sensor. *Journal of Solid State Electrochemistry* 22 (1):169–80. doi: 10.1007/s10008-017-3731-z.

Shang, L., F. Q. Zhao, and B. Z. Zeng. 2014. 3D Porous graphene-porous PdCu alloy nanoparticles-molecularly imprinted poly(*para*-aminobenzoic acid) composite for the electrocatalytic assay of melamine. *ACS Applied Materials & Interfaces* 6 (21):18721–7. doi: 10.1021/am504276g.

Sharma, P. S., M. Dabrowski, F. D'Souza, and W. Kutner. 2013. Surface development of molecularly imprinted polymer films to enhance sensing signals. *TrAC: Trends in Analytical Chemistry* 51:146–57. doi: 10.1016/j.trac.2013.07.006.

Sharma, P. S., A. Garcia-Cruz, M. Cieplak, K. R. Noworyta, and W. Kutner. 2019. Gate effect' in molecularly imprinted polymers: The current state of understanding. *Current Opinion in Electrochemistry* 16:50–6. doi: 10.1016/j.coelec.2019.04.020.

Sharma, P. S., A. Pietrzyk-Le, F. D'Souza, and W. Kutner. 2012. Electrochemically synthesized polymers in molecular imprinting for chemical sensing. *Analytical and Bioanalytical Chemistry* 402 (10):3177–204. doi: 10.1007/s00216-011-5696-6.

Shi, X. J., J. X. Lu, H. Z. Yin, X. G. Qiao, and Z. X. Xu. 2017. A biomimetic sensor with signal enhancement of ferriferrous oxide-reduced graphene oxide nanocomposites for ultratrace levels quantification of methamidophos or omethoate in vegetables. *Food Analytical Methods* 10 (4):910–20. doi: 10.1007/s12161-016-0641-0.

Shirani, M. P., B. Rezaei, A. A. Ensafi, and M. Ramezani. 2021. Development of an eco-friendly fluorescence nanosensor based on molecularly imprinted polymer on silica-carbon quantum dot for the rapid indoxacarb detection. *Food Chemistry* 339:127920. doi: 10.1016/j.foodchem.2020.127920.

Shirzadmehr, A., A. Afkhami, and T. Madrakian. 2015. A new nano-composite potentiometric sensor containing an Hg^{2+}-ion imprinted polymer for the trace determination of mercury ions in different matrices. *Journal of Molecular Liquids* 204:227–35. doi: 10.1016/j.molliq.2015.01.014.

Siciliano, G., A. G. Monteduro, A. Turco, E. Primiceri, S. Rizzato, N. Depalo, M. L. Curri, and G. Maruccio. 2022. Polydopamine-coated magnetic iron oxide nanoparticles: From design to applications. *Nanomaterials* 12 (7):1145. doi: 10.3390/nano12071145.

Silva, P., J. Freitas, F. M. Nunes, and J. S. Camara. 2021. A predictive strategy based on volatile profile and chemometric analysis for traceability and authenticity of sugarcane honey on the global market. *Foods* 10 (7):1559. doi: 10.3390/foods10071559.

Silva, P., C. L. Silva, R. Perestrelo, F. M. Nunes, and J. S. Camara. 2018. Fingerprint targeted compounds in authenticity of sugarcane honey - An approach based on chromatographic and statistical data. *LWT* 96:82–9. doi: 10.1016/j.lwt.2018.04.076.

Singathi, R., R. Raghunathan, R. Krishnan, S. Kumar Rajendran, S. Baburaj, Mukund, P. Sibi, D. C. Webster, and J. Sivaguru. 2022. Towards upcycling biomass-derived crosslinked polymers with light. *Angewandte Chemie International Edition* 22:e202203353.

Song, B., Y. S. Zhou, H. Jin, T. Jing, T. T. Zhou, Q. L. Hao, Y. K. Zhou, S. R. Mei, and Y. I. Lee. 2014. Selective and sensitive determination of erythromycin in honey and dairy products by molecularly imprinted polymers based electrochemical sensor. *Microchemical Journal* 116:183–90. doi: 10.1016/j.microc.2014.05.010.

Soon, J. M., S. C. Krzyzaniak, Z. Shuttlewood, M. Smith, and L. Jack. 2019. Food fraud vulnerability assessment tools used in food industry. *Food Control* 101:225–32. doi: 10.1016/j.foodcont.2019.03.002.

Sun, A., J. Chai, T. Xiao, X. Shi, X. Li, Q. Zhao, D. Li, and J. Chen. 2018. Development of a selective fluorescence nanosensor based on molecularly imprinted-quantum dot optosensing materials for saxitoxin detection in shellfish samples. *Sensors and Actuators B: Chemical* 258:408–14. doi: 10.1016/j.snb.2017.11.143.

Sun, S., M. Q. Zhang, Y. J. Li, and X. W. He. 2013. A molecularly imprinted polymer with incorporated graphene oxide for electrochemical determination of quercetin. *Sensors (Basel, Switzerland)* 13 (5):5493–506. doi: 10.3390/s130505493.

Susanti, I., and A. N. Hasanah. 2021. How to develop molecularly imprinted mesoporous silica for selective recognition of analytes in pharmaceutical, environmental, and food samples. *Polymers for Advanced Technologies* 32 (5):1965–80. doi: 10.1002/pat.5251.

Susanti, I., M. Mutakin, and A. N. Hasanah. 2022. Factors affecting the analytical performance of molecularly imprinted mesoporous silica. *Polymers for Advanced Technologies* 33 (2):469–83. doi: 10.1002/pat.5545.

Tarannum, N., S. Khatoon, and B. B. Dzantiev. 2020. Perspective and application of molecular imprinting approach for antibiotic detection in food and environmental samples: A critical review. *Food Control* 118:107381. doi: 10.1016/j.foodcont.2020.107381.

Turco, A., S. Corvaglia, and E. Mazzotta. 2015. Electrochemical sensor for sulfadimethoxine based on molecularly imprinted polypyrrole: Study of imprinting parameters. *Biosensors & Bioelectronics* 63:240–7. doi: 10.1016/j.bios.2014.07.045.

Turco, A., S. Corvaglia, E. Mazzotta, P. P. Pompa, and C. Malitesta. 2018. Preparation and characterization of molecularly imprinted mussel inspired film as antifouling and selective layer for electrochemical detection of sulfamethoxazole. *Sensors and Actuators B: Chemical* 255:3374–83. doi: 10.1016/j.snb.2017.09.164.

Turiel, E., and A. Martin-Esteban. 2010. Molecularly imprinted polymers for sample preparation: A review. *Analytica Chimica Acta* 668 (2):87–99.

Uzun, L., and A. P. F. Turner. 2016. Molecularly-imprinted polymer sensors: Realising their potential. *Biosensors & Bioelectronics* 76:131–44. doi: 10.1016/j.bios.2015.07.013.

Valero-Navarro, A., M. Gomez-Romero, J. F. Fernandez-Sanchez, P. A. G. Cormack, A. Segura-Carretero, and A. Fernandez-Gutierrez. 2011. Synthesis of caffeic acid molecularly imprinted polymer microspheres and high-performance liquid chromatography evaluation of their sorption properties. *Journal of Chromatography A* 1218 (41):7289–96. doi: 10.1016/j.chroma.2011.08.043.

Wackerlig, J., and P. A. Lieberzeit. 2015. Molecularly imprinted polymer nanoparticles in chemical sensing - Synthesis, characterisation and application. *Sensors and Actuators B: Chemical* 207:144–57. doi: 10.1016/j.snb.2014.09.094.

Wang, D., S. Jiang, Y. Liang, X. Wang, X. Zhuang, C. Tian, F. Luan, and L. Chen. 2022. Selective detection of enrofloxacin in biological and environmental samples using a molecularly imprinted electrochemiluminescence sensor based on functionalized copper nanoclusters. *Talanta* 236:122835. doi: 10.1016/j.talanta.2021.122835.

Wang, H. W., S. Yao, Y. Q. Liu, S. L. Wei, J. W. Su, and G. X. Hu. 2017. Molecularly imprinted electrochemical sensor based on Au nanoparticles in carboxylated multi-walled carbon nanotubes for sensitive determination of olaquindox in food and feedstuffs. *Biosensors & Bioelectronics* 87:417–21. doi: 10.1016/j.bios.2016.08.092.

Wang, J., J. Y. Li, C. Zeng, Q. Qu, M. F. Wang, W. Qi, R. X. Su, and Z. M. He. 2020. Sandwich-like sensor for the highly specific and reproducible detection of Rhodamine 6G on a surface-enhanced Raman scattering platform. *ACS Applied Materials & Interfaces* 12 (4):4699–706. doi: 10.1021/acsami.9b16773.

Wang, Q. H., G. Z. Fang, Y. Y. Liu, D. D. Zhang, J. M. Liu, and S. Wang. 2017. Fluorescent sensing probe for the sensitive detection of histamine based on molecular imprinting ionic liquid-modified quantum dots. *Food Analytical Methods* 10 (7):2585–92. doi: 10.1007/s12161-017-0795-4.

Wen, Z., D. Gao, J. Lin, S. Li, K. Zhang, Z. Xia, and D. Wang. 2022. Magnetic porous cellulose surface-imprinted polymers synthetized with assistance of deep eutectic solvent for specific recognition and purification of bisphenols. *International Journal of Biological Macromolecules* 216:374–87. doi: 10.1016/j.ijbiomac.2022.06.187.

Wijayaratne, S. P., M. Reid, K. Westberg, A. Worsley, and F. Mavondo. 2018. Food literacy, healthy eating barriers and household diet. *European Journal of Marketing* 52 (12):2449–77. doi: 10.1108/EJM-10-2017-0760.

Wolff, T., and H. Görner. 2010. Photocleavage of dimers of coumarin and 6-alkylcoumarins. *Journal of Photochemistry and Photobiology A: Chemistry* 209 (2–3):219–23. doi: 10.1016/j.jphotochem.2009.11.018.

Wu, L., Z. Z. Lin, H. P. Zhong, X. M. Chen, and Z. Y. Huang. 2017. Rapid determination of malachite green in water and fish using a fluorescent probe based on CdTe quantum dots coated with molecularly imprinted polymer. *Sensors and Actuators B: Chemical* 239:69–75. doi: 10.1016/j.snb.2016.07.166.

Wu, M., H. Y. Deng, Y. J. Fan, Y. C. Hu, Y. P. Guo, and L. W. Xie. 2018. Rapid colorimetric detection of cartap residues by AgNP sensor with magnetic molecularly imprinted microspheres as recognition elements. *Molecules* 23 (6):1443. doi: 10.3390/molecules23061443.

Wu, W. H., L. T. Yang, F. Q. Zhao, and B. Z. Zeng. 2017. A vanillin electrochemical sensor based on molecularly imprinted poly(1-vinyl-3-octylimidazole hexafluoride phosphorus)-multi-walled carbon nanotubes@polydopamine-carboxyl single-walled carbon nanotubes composite. *Sensors and Actuators B: Chemical* 239:481–7. doi: 10.1016/j.snb.2016.08.041.

Wu, W. Z., M. X. Huang, Q. D. Huang, C. H. Lyu, J. P. Lai, and H. Sun. 2019. Molecularly imprinted photonic hydrogels for visual detection of methylanthranilate in wine. *Chinese Journal of Analytical Chemistry* 47 (9):1330–6. doi: 10.1016/S1872-2040(19)61188-6.

Wu, Z. Z., E. B. Xu, J. P. Li, J. Long, A. Q. Jiao, and Z. Y. Jin. 2016. Highly sensitive determination of ethyl carbamate in alcoholic beverages by surface-enhanced Raman spectroscopy combined with a molecular imprinting polymer. *RSC Advances* 6 (111):109442–52. doi: 10.1039/C6RA23165A.

Xiao, L., Z. Zhang, C. C. Wu, L. Y. Han, and H. Y. Zhang. 2017. Molecularly imprinted polymer grafted paper-based method for the detection of 17 beta-estradiol. *Food Chemistry* 221:82–6. doi: 10.1016/j.foodchem.2016.10.062.

Xie, Y., M. Zhao, Q. Hu, Y. Cheng, Y. Guo, H. Qian, and W. Yao. 2017. Selective detection of chloramphenicol in milk based on a molecularly imprinted polymer-surface-enhanced Raman spectroscopic nanosensor. *Journal of Raman Spectroscopy* 48 (2):204–10. doi: 10.1002/jrs.5034.

Xu, G., Y. Chi, L. Li, S. Liu, and X. Kan. 2015. Imprinted propyl gallate electrochemical sensor based on graphene/single walled carbon nanotubes/sol-gel film. *Food Chemistry* 177:37–42. doi: 10.1016/j.foodchem.2014.12.097.

Xu, J. J., S. Ambrosini, E. Tamahkar, C. Rossi, K. Haupt, and B. T. S. Bui. 2016. Toward a universal method for preparing molecularly imprinted polymer nanoparticles with antibody-like affinity for proteins. *Biomacromolecules* 17 (1):345–53. doi: 10.1021/acs.biomac.5b01454.

Xu, S., G. Y. Lin, W. Zhao, Q. Wu, J. Luo, W. Wei, X. Y. Liu, and Y. Zhu. 2018. Necklace-like molecularly imprinted nanohybrids based on polymeric nanoparticles decorated multiwalled carbon nanotubes for highly sensitive and selective melamine detection. *ACS Applied Materials & Interfaces* 10 (29):24850–9. doi: 10.1021/acsami.8b08558.

Yang, G. M., and F. Q. Zhao. 2015. Electrochemical sensor for dimetridazole based on novel gold nanoparticles@molecularly imprinted polymer. *Sensors and Actuators B: Chemical* 220:1017–22. doi: 10.1016/j.snb.2015.06.051.

Yang, L. T., B. J. Xu, H. L. Ye, F. Q. Zhao, and B. Z. Zeng. 2017. A novel quercetin electrochemical sensor based on molecularly imprinted poly(para-aminobenzoic acid) on 3D Pd nanoparticles-porous graphene-carbon nanotubes composite. *Sensors and Actuators B: Chemical* 251:601–8. doi: 10.1016/j.snb.2017.04.006.

Yang, L. T., F. Q. Zhao, and B. Z. Zeng. 2016. Electrochemical determination of eugenol using a three-dimensional molecularly imprinted poly (p-aminothiophenol-co-p-aminobenzoic acids) film modified electrode. *Electrochimica Acta* 210:293–300. doi: 10.1016/j.electacta.2016.05.167.

Yang, Q., H. L. Peng, J. H. Li, Y. B. Li, H. Xiong, and L. X. Chen. 2017. Label-free colorimetric detection of tetracycline using analyte-responsive inverse-opal hydrogels based on molecular imprinting technology. *New Journal of Chemistry* 41 (18):10174–80. doi: 10.1039/C7NJ02368E.

Yao, G. H., R. P. Liang, C. F. Huang, Y. Wang, and J. D. Qiu. 2013. Surface plasmon resonance sensor based on magnetic molecularly imprinted polymers amplification for pesticide recognition. *Analytical Chemistry* 85 (24):11944–51. doi: 10.1021/ac402848x.

Yao, T., X. Gu, T. Li, J. Li, J. Li, Z. Zhao, J. Wang, Y. Qin, and Y. She. 2016. Enhancement of surface plasmon resonance signals using a MIP/GNPs/rGO nano-hybrid film for the rapid detection of ractopamine. *Biosensors & Bioelectronics* 75:96–100. doi: 10.1016/j.bios.2015.08.027.

Ye, T., W. Yin, N. Zhu, M. Yuan, H. Cao, J. Yu, Z. Gou, X. Wang, H. Zhu, A. Reyihanguli, et al. 2018. Colorimetric detection of pyrethroid metabolite by using surface molecularly imprinted polymer. *Sensors and Actuators B: Chemical* 254:417–23. doi: 10.1016/j.snb.2017.07.132.

Yin, W. M., L. Wu, F. Ding, Q. Li, P. Wang, J. J. Li, Z. C. Lu, and H. Y. Han. 2018. Surface-imprinted SiO_2@Ag nanoparticles for the selective detection of BPA using surface enhanced Raman scattering. *Sensors and Actuators B: Chemical* 258:566–73. doi: 10.1016/j.snb.2017.11.141.

Yin, Z.-Z., S.-W. Cheng, L.-B. Xu, H.-Y. Liu, K. Huang, L. Li, Y.-Y. Zhai, Y.-B. Zeng, H.-Q. Liu, Y. Shao, et al. 2018. Highly sensitive and selective sensor for sunset yellow based on molecularly imprinted polydopamine-coated multi-walled carbon nanotubes. *Biosensors & Bioelectronics* 100:565–70. doi: 10.1016/j.bios.2017.10.010.

You, A. M., Y. H. Cao, and G. Q. Cao. 2016. Colorimetric sensing of melamine using colloidal magnetically assembled molecularly imprinted photonic crystals. *RSC Advances* 6 (87):83663–7. doi: 10.1039/C6RA18617C.

You, A. M., X. J. Ni, Y. H. Cao, and G. Q. Cao. 2017. Colorimetric chemosensor for chloramphenicol based on colloidal magnetically assembled molecularly imprinted photonic crystals. *Journal of the Chinese Chemical Society* 64 (10):1235–41. doi: 10.1002/jccs.201700126.

Zahara, S., M. A. Minhas, H. Shaikh, M. S. Ali, M. I. Bhanger, and M. I. Malik. 2021. Molecular imprinting-based extraction of rosmarinic acid from Salvia hypoleuca extract. *Reactive and Functional Polymers* 166:104984. doi: 10.1016/j.reactfunctpolym.2021.104984.

Zhang, L. L., C. C. Zhu, C. B. Chen, S. H. Zhu, J. Zhou, M. L. Wang, and P. P. Shang. 2018. Determination of kanamycin using a molecularly imprinted SPR sensor. *Food Chemistry* 266:170–4. doi: 10.1016/j.foodchem.2018.05.128.

Zhang, M., H. T. Zhao, T. J. Xie, X. Yang, A. J. Dong, H. Zhang, J. Wang, and Z. Y. Wang. 2017. Molecularly imprinted polymer on graphene surface for selective and sensitive electrochemical sensing imidacloprid. *Sensors and Actuators B: Chemical* 252:991–1002. doi: 10.1016/j.snb.2017.04.159.

Zhang, R.-R., X.-T. Gan, J.-J. Xu, Q.-F. Pan, H. Liu, A.-L. Sun, X.-Z. Shi, and Z.-M. Zhang. 2022. Ultrasensitive electrochemiluminescence sensor based on perovskite quantum dots coated with molecularly imprinted polymer for prometryn determination. *Food Chemistry* 370:131353. doi: 10.1016/j.foodchem.2021.131353.

Zhang, Z. H., R. Cai, F. Long, and J. Wang. 2015. Development and application of tetrabromobisphenol A imprinted electrochemical sensor based on graphene/carbon nanotubes three-dimensional nanocomposites modified carbon electrode. *Talanta* 134:435–42. doi: 10.1016/j.talanta.2014.11.040.

Zhao, B. W., S. L. Feng, Y. X. Hu, S. Wang, and X. N. Lu. 2019. Rapid determination of atrazine in apple juice using molecularly imprinted polymers coupled with gold nanoparticles-colorimetric/SERS dual chemosensor. *Food Chemistry* 276:366–75. doi: 10.1016/j.foodchem.2018.10.036.

Zhao, P. N., H. Y. Liu, L. N. Zhang, P. H. Zhu, S. G. Ge, and J. H. Yu. 2020. Paper-based SERS sensing platform based on 3D silver dendrites and molecularly imprinted identifier sandwich hybrid for neonicotinoid quantification. *ACS Applied Materials & Interfaces* 12 (7):8845–54. doi: 10.1021/acsami.9b20341.

Zhao, X. L., Y. He, Y. N. Wang, S. Wang, and J. P. Wang. 2020. Hollow molecularly imprinted polymer based quartz crystal microbalance sensor for rapid detection of methimazole in food samples. *Food Chemistry* 309:125787. doi: 10.1016/j.foodchem.2019.125787.

Zhao, Y., L. Tian, X. Zhang, Z. Sun, X. Shan, Q. Wu, R. Chen, and J. Lu. 2022. A novel molecularly imprinted polymer electrochemiluminescence sensor based on Fe_2O_3@$Ru(bpy)_3^{2+}$ for determination of clenbuterol. *Sensors and Actuators B: Chemical* 350:130822. doi: 10.1016/j.snb.2021.130822.

Zhou, J. Y., S. Sheth, H. F. Zhou, and Q. J. Song. 2020. Highly selective detection of L-Phenylalanine by molecularly imprinted polymers coated Au nanoparticles via surface-enhanced Raman scattering. *Talanta* 211:120745. doi: 10.1016/j.talanta.2020.120745.

Zouaoui, F., S. Bourouina-Bacha, M. Bourouina, N. Jaffrezic-Renault, N. Zine, and A. Errachid. 2020. Electrochemical sensors based on molecularly imprinted chitosan: A review. *TrAC: Trends in Analytical Chemistry* 130:115982. doi: 10.1016/j.trac.2020.115982.

Zoughi, S., F. Faridbod, A. Amiri, and M. R. Ganjali. 2021. Detection of tartrazine in fake saffron containing products by a sensitive optical nanosensor. *Food Chemistry* 350:129197. doi: 10.1016/j.foodchem.2021.129197.